

Inf²Guard: An Information-Theoretic Framework for Learning Privacy-Preserving Representations against Inference Attacks

Sayedeh Leila Noorbakhsh^{1,*}, Binghui Zhang^{1,*}, Yuan Hong², Binghui Wang¹
¹*Illinois Institute of Technology*, ²*University of Connecticut*, **Equal contribution*

Abstract

Machine learning (ML) is vulnerable to inference (e.g., membership inference, property inference, and data reconstruction) attacks that aim to infer the private information of training data or dataset. Existing defenses are only designed for one specific type of attack and sacrifice significant utility or are soon broken by adaptive attacks. We address these limitations by proposing an information-theoretic defense framework, called Inf²Guard, against the three major types of inference attacks. Our framework, inspired by the success of representation learning, posits that learning shared representations not only saves time/costs but also benefits numerous downstream tasks. Generally, Inf²Guard involves two mutual information objectives, for privacy protection and utility preservation, respectively. Inf²Guard exhibits many merits: it facilitates the design of customized objectives against the specific inference attack; it provides a general defense framework which can treat certain existing defenses as special cases; and importantly, it aids in deriving theoretical results, e.g., inherent utility-privacy tradeoff and guaranteed privacy leakage. Extensive evaluations validate the effectiveness of Inf²Guard for learning privacy-preserving representations against inference attacks and demonstrate the superiority over the baselines.¹

1 Introduction

Machine learning (ML) models (particularly deep neural networks) are vulnerable to inference attacks, which aim to infer sensitive information about the training data/dataset that are used to train the models. There are three well-known types of inference attacks on training data/dataset: membership inference attacks (MIAs) [13, 61, 76], property inference attacks (PIAs) (also called distribution inference attacks) [6, 22, 66], and data reconstruction attacks (DRAs) (also called model inversion attacks) [7, 31]. Given an ML model, in MIAs, an adversary aims to infer whether a particular data sample was in the training set, while in PIAs, an adversary aims to infer

statistical properties of the training dataset used to train the targeted ML model. Furthermore, an adversary aims to directly reconstruct the training data in DRAs. Leaking the data sample or information about the dataset raises serious privacy issues. For instance, by performing MIAs, an adversary is able to identify users included in sensitive medical datasets, which itself is a privacy violation [33]. By performing PIAs, an adversary can determine whether or not machines that generated the bitcoin logs were patched for Meltdown and Spectre attacks [22]. More seriously, DRAs performed by an adversary leak all the information about the training data.

To mitigate the privacy risks, various defenses have been proposed against MIAs [38, 48, 57, 59, 61, 62, 64, 74] and DRAs [23, 28, 41, 51, 58, 65, 72, 84]². However, there are two fundamental limitations in existing defenses: 1) They are designed against only one specific type of attack; 2) Provable defenses (based on differential privacy [3, 20]) incur significant utility losses to achieve reasonable defense performance against inference attacks [36, 59] since the design of such randomization-based defenses did not consider specific inference attacks (also see Section 5); and empirical defenses are soon broken by stronger/adaptive attacks [9, 17, 62].

We aim to address these limitations and consider the question: 1) *Can we design a unified privacy protection framework against these inference attacks, that also maintain utility?* 2) *Under the framework, can we further theoretically understand the utility-privacy tradeoff and the privacy leakage against the inference attacks?* To this end, we propose an information-theoretic defense framework, termed Inf²Guard, against inference attacks through the lens of *representation learning* [11]. Representation learning has been one of the biggest successes in modern ML/AI so far (e.g., it plays an important role in today’s large language models such as ChatGPT [1] and PaLM2 [2]). Particularly, rather than training large models from scratch, which requires huge computational costs and time (e.g., GPT-3 has 175 billion parameters), learn-

¹Source code: <https://github.com/leilynorbakhsh/Inf2Guard>.

²To our best knowledge, there exist no effective defenses against PIAs. [29] analyzes sources of information leakage to cause PIAs, but their solutions are difficult to be tested on real-world datasets due to lack of generality.

ing shared representations (or pretrained encoder)³ presents an economical alternative. For instance, the shared representations can be directly used or further fine-tuned with different purposes, achieving considerable savings in time and cost.

More specifically, we formulate Inf^2Guard via two mutual information (MI)⁴ objectives in general, for privacy protection and utility preservation, respectively. Under this framework, we can design customized MI objectives to defend against each inference attack. For instance, to defend against MIAs, we design one MI objective to learn representations that contain as less information as possible about the membership of the training data—thus protecting membership privacy, while the other one to ensure the learnt representations include as much information as possible about the training data labels—thus maintaining utility. However, directly solving the MI objectives for each inference attack is challenging, since calculating an MI between arbitrary variables is often infeasible [52]. To address it, we are inspired by the MI neural estimation [4, 10, 16, 32, 50, 53], which transfers the intractable MI calculations to the tractable variational MI bounds. Then, we are capable of parameterizing each bound with a (deep) neural network, and train neural networks to approximate the true MI and learn representations against the inference attacks. Finally, we can derive theoretical results based on our MI objectives: we obtain an inherent utility-privacy tradeoff, and guaranteed privacy leakage against each inference attack.

We extensively evaluate Inf^2Guard and compare it with the existing defenses against the inference attacks on multiple benchmark datasets. Our experimental results validate that Inf^2Guard obtains a promising utility-privacy tradeoff and significantly outperforms the existing defenses. For instance, under the same defense performance against MIAs, Inf^2Guard has a 30% higher testing accuracy than the DP-SGD [3]. Our results also validate the privacy-utility tradeoffs obtained by Inf^2Guard ⁵.

Our main contributions are summarized as below:

- **Algorithm:** We design the first unified framework Inf^2Guard to defend against the three well-known types of inference attacks via information theory. Our framework can instantiate many existing defenses as special cases, e.g., AdvReg [48] against MIAs (See Section 3.1) and Soteria [65] against DRAs (See Section 3.3).
- **Theory:** Based on our formulation, we can derive novel theoretical results, e.g., the inherent tradeoff between utility and privacy, and guaranteed privacy leakage against all the considered inference attacks.

³Pretrained encoder as a service has been widely deployed by industry, e.g., OpenAI’s GPT-4 API [1] and Clarifai’s Embedding API [18]. We will interchangeably use the pretrained encoder and learnt representations.

⁴In information theory, MI is a measure of shared information between random variables, and offers a metric to quantify the “amount of information” obtained about one random variable by observing the other random variable.

⁵A recent work [56] formulates defenses against inference attacks under a privacy game framework, but it does not propose concrete defense solutions.

- **Evaluation:** Extensive evaluations verify the effectiveness of Inf^2Guard for learning privacy-preserving representations against inference attacks.

2 Background and Problem Definition

Notations: We use s , \mathbf{s} , \mathbf{S} , and \mathcal{S} to denote (random) scalar, vector, matrix, and space, respectively. Accordingly, $\Pr(s)$, $\Pr(\mathbf{s})$, and $\Pr(\mathbf{S})$ are the probability distribution over s , \mathbf{s} , and \mathbf{S} . $I(\mathbf{x}; \mathbf{r})$ and $H(\mathbf{x}, \mathbf{r})$ are the mutual information and cross entropy between a pair of random variables (\mathbf{x}, \mathbf{r}) , respectively, and $H(\mathbf{x}) = I(\mathbf{x}; \mathbf{x})$ as the entropy of \mathbf{x} . $KL(p||q)$ is the KL-divergence between two distributions p and q . We denote \mathcal{D} as the underlying distribution that data are sampled from. A data sample is denoted as $(\mathbf{x}, y) \sim \mathcal{D}$, where $\mathbf{x} \in \mathcal{X}$ is data features, $y \in \mathcal{Y}$ is the label, and \mathcal{X} and \mathcal{Y} are the data space and label space, respectively. We further denote a dataset as $D = \{\mathbf{X}, \mathbf{y}\} = \{(\mathbf{x}_i, y_i)\}$, that consists of a set of data samples $(\mathbf{x}_i, y_i) \sim \mathcal{D}$, and will interchangeably use D and $\{\mathbf{X}, \mathbf{y}\}$. We let $u \in \mathcal{U}$ be the private attribute within the attribute space \mathcal{U} . For instance, in MIAs, $u \in \mathcal{U} = \{0, 1\}$ means a binary-valued private membership; in PIAs, $u \in \mathcal{U} = \{1, 2, \dots, K\}$ indicates a K -valued private dataset property; and $u \in \mathcal{U} = \mathcal{X}$ indicates the private data itself in DRAs. The composition function of two functions f and g is denoted as $(g \circ f)(\cdot) = g(f(\cdot))$.

2.1 Formalizing Privacy Attacks

We denote a classification model⁶ $F_\theta : \mathcal{X} \rightarrow \mathcal{Y}$ as a function, parameterized by θ , that maps a data sample $\mathbf{x} \in \mathcal{X}$ to a label $y \in \mathcal{Y}$. Given a training set $D \sim \mathcal{D}$, we denote $F \leftarrow \mathcal{T}(D)$ as learned by running a training algorithm \mathcal{T} on the dataset D .

Formalizing MIAs: Assume a data sample $(\mathbf{x}, y) \sim \mathcal{D}$ with a private membership u that is chosen uniformly at random from $\{0, 1\}$, where $u = 1$ means (\mathbf{x}, y) is a member of D , and 0 otherwise. An MIA A_{MIA} has access to \mathcal{D} and F , takes (\mathbf{x}, y) as input, and outputs a binary $A_{MIA}^{\mathcal{D}, F}(\mathbf{x}, y)$. We omit \mathcal{D}, F for notation simplicity. Then, the attack performance of an MIA A_{MIA} is defined as $\Pr_{(\mathbf{x}, y, u)}(A_{MIA}(\mathbf{x}, y) = u)$.

Formalizing PIAs: PIAs define a private property on a dataset. Given a dataset $D_u \sim \mathcal{D}$ with a private property u chosen uniformly at random from $\{1, 2, \dots, K\}$. A PIA A_{PIA} has access to \mathcal{D} and F , and outputs a K -valued $A_{PIA}(D_u)$. Then, the attack performance of a PIA A_{PIA} is defined as $\Pr_{(D_u, u)}(A_{PIA}(D_u) = u)$.

Formalizing DRAs: Given a random data $(\mathbf{x}, y) \in D$, DRAs aim to reconstruct the private \mathbf{x} . A DRA A_{DRA} has access to \mathcal{D} and F , and outputs a reconstructed $\hat{\mathbf{x}} = A_{DRA}(\mathbf{x}, y)$. The DRA performance is measured by the similarity/difference between $\hat{\mathbf{x}}$ and \mathbf{x} . For instance, [7] introduces the (η, γ) -reconstruction metric defined as $\Pr_{(\mathbf{x}, y)}(\|\hat{\mathbf{x}} - \mathbf{x}\|_2 \leq \eta) \geq \gamma$, where a smaller η and a larger γ imply a more severe DRA.

⁶In this paper, we focus on classification models for simplicity.

2.2 Threat Model and Problem Formulation

We have three roles: *task learner*, *defender*, and *attacker*. The task learner (i.e., data owner) aims to learn an accurate classification model on its training data. The defender (e.g., data owner or a trusted service provider) aims to protect the training data privacy—it designs a defense framework by learning *shared data representations* that are robust against inference attacks. The attacker can *arbitrarily* use data representations to perform the inference attack. The attacker is also assumed to know the underlying data distribution, but cannot access the internal encoder (e.g., deployed as an API [1, 18]).

Formally, we denote $f_{\Theta} : \mathcal{X} \rightarrow \mathcal{Z}$ as the *encoder*, parameterized by Θ , that maps a data sample $\mathbf{x} \in \mathcal{X}$ (or a dataset $\mathbf{X} \in \mathcal{X}$) to its representation vector $\mathbf{r} = f(\mathbf{x}) \in \mathcal{Z}$ (or representation matrix $\mathbf{R} = f(\mathbf{X}) \in \mathcal{Z}$), where \mathcal{Z} is the representation space. Moreover, we let $C : \mathcal{Z} \rightarrow \mathcal{Y}$ be the *classification model* on top of the representation \mathbf{r} or encoder f , which predicts the data label y (or dataset labels \mathbf{y}). We further let $A : \mathcal{Z} \rightarrow \mathcal{U}$ be the *inference model*, which infers the private attribute u using the learnt representations \mathbf{r} or \mathbf{R} . Then, our defense goals are:

- **Defend against MIAs:** Given a random sample $(\mathbf{x}, y, u) \in \mathcal{D}$, we expect to learn f such that the MIA performance $\Pr(A_{MIA}(f(\mathbf{x}), y) = u)$ is low, and the utility loss/risk, i.e., $\text{Risk}_{MIA}(C \circ f) = \Pr(C \circ f(\mathbf{x}) \neq y)$, is also small.
- **Defend against PIAs:** Given a random dataset $(\mathbf{X}, \mathbf{y}, u) \in \mathcal{D}$, we expect to learn f with low PIA performance $\Pr(A_{PIA}(f(\mathbf{X}), \mathbf{y}) = u)$, and also a small utility loss/risk, i.e., $\text{Risk}_{PIA}(C \circ f) = \frac{1}{|\mathcal{Y}|} \sum_{(\mathbf{x}, y) \in \{\mathbf{X}, \mathbf{y}\}} \Pr(C \circ f(\mathbf{x}) \neq y)$.
- **Defend against DRAs:** Given a random sample $(\mathbf{x}, y) \in \mathcal{D}$, we expect to learn f with low DRA performance, i.e., $\Pr_{(\mathbf{x}, y)}(\|\hat{\mathbf{x}} - \mathbf{x}\|_2 \geq \eta) \geq \gamma$ with a large η and γ (flipping the inequality direction on η for DRAs), and also a small utility risk $\text{Risk}_{DRA}(C \circ f) = \Pr(C \circ f(\mathbf{x}) \neq y)$.

3 Design of Inf²Guard

3.1 Inf²Guard against MIAs

3.1.1 MI objectives

Given a data sample $\mathbf{x} \sim \mathcal{D}$, from the training set D (i.e., $u = 1$) or not (i.e., $u = 0$), the defender learns the representation $\mathbf{r} = f(\mathbf{x})$ that satisfies the following two goals:

- **Goal 1: Membership protection.** \mathbf{r} contains as less information as possible about the private membership u . Ideally, when \mathbf{r} does not include information about u (i.e., $\mathbf{r} \perp u$), it is impossible to infer u from \mathbf{r} . Formally, we quantify the membership protection using the MI objective as follows:

$$\min_f I(\mathbf{r}; u), \quad (1)$$

where we minimize such MI to maximally reduce the correlation between \mathbf{r} and u .

- **Goal 2: Utility preservation.** \mathbf{r} should be effective for predicting the label y of the *training* data (i.e., $u = 1$), thus preserving utility. Formally, we quantify the utility preservation using the below MI objective:

$$\max_f I(y; \mathbf{r} | u = 1), \quad (2)$$

where we maximize such MI to make \mathbf{r} accurately predict the training data label y during training.

3.1.2 Estimating MI via tractable bounds

The key challenge of solving the above two MI objectives is that calculating an MI between two arbitrary random variables is likely to be infeasible [52]. Inspired by the existing MI neural estimation methods [4, 10, 16, 32, 50, 53], we convert the intractable exact MI calculations to the tractable variational MI bounds. Specifically, we first obtain an MI upper bound for membership protection and an MI lower bound for utility preserving via introducing two auxiliary posterior distributions, respectively. Then, we parameterize each auxiliary distribution with a neural network, and approximate the true MI by minimizing the upper bound and maximizing the lower bound through training the involved neural networks. *We emphasize we do not design novel MI neural estimators, but adopt existing ones to assist our MI objectives for learning privacy-preserving representations. Note that, though the estimated MI bounds may not be tight (due to the MI estimators or auxiliary distributions learnt by neural networks) [16, 32], they have shown promising performance in practice. It is still an active research topic to design better MI estimators that lead to tighter MI bounds (which is orthogonal to this work).*

Minimizing the upper bound MI in Equation (1). We adapt the variational upper bound proposed in [16]. Specifically,

$$I(\mathbf{r}; u) \leq I_{VCLUB}(\mathbf{r}; u) = \mathbb{E}_{p(\mathbf{r}, u)} [\log q_{\Psi}(u|\mathbf{r})] - \mathbb{E}_{p(\mathbf{r})p(u)} [\log q_{\Psi}(u|\mathbf{r})],$$

where $q_{\Psi}(u|\mathbf{r})$ is an auxiliary posterior distribution of $p(u|\mathbf{r})$ needing to satisfy the below condition on KL divergence: $KL(p(\mathbf{r}, u) \| q_{\Psi}(\mathbf{r}, u)) \leq KL(p(\mathbf{r})p(u) \| q_{\Psi}(\mathbf{r}, u))$. To achieve this, we thus minimize:

$$\begin{aligned} \min_{\Psi} KL(p(\mathbf{r}, u) \| q_{\Psi}(\mathbf{r}, u)) &= \min_{\Psi} KL(p(u|\mathbf{r}) \| q_{\Psi}(u|\mathbf{r})) \\ &= \min_{\Psi} \mathbb{E}_{p(\mathbf{r}, u)} [\log p(u|\mathbf{r})] - \mathbb{E}_{p(\mathbf{r}, u)} [\log q_{\Psi}(u|\mathbf{r})] \\ &\iff \max_{\Psi} \mathbb{E}_{p(\mathbf{r}, u)} [\log q_{\Psi}(u|\mathbf{r})], \end{aligned} \quad (3)$$

where we note that $\mathbb{E}_{p(\mathbf{r}, u)} [\log p(u|\mathbf{r})]$ is irrelevant to Ψ . [16] proved when $q_{\Psi}(u|\mathbf{r})$ is parameterized by a neural network with high expressiveness (e.g., deep neural network), the condition is satisfied almost surely by maximizing Equation (3). Finally, our **Goal 1** for privacy protection is reformulated as solving the below *min-max* objective function:

$$\min_f \min_{\Psi} I_{VCLUB}(\mathbf{r}; u) \iff \min_f \max_{\Psi} \mathbb{E}_{p(\mathbf{r}, u)} [\log q_{\Psi}(u|\mathbf{r})] \quad (4)$$

Remark. Equation (4) can be interpreted as an *adversarial game* between an adversary q_Ψ (i.e., a membership inference classifier) who aims to infer the membership u from \mathbf{r} ; and the encoder f who aims to protect u from being inferred.

Maximizing the lower bound MI in Equation (2). We adopt the MI estimator proposed in [49] to estimate the lower bound of Equation (2). Specifically, we have

$$\begin{aligned} I(y; \mathbf{r} | u = 1) &= H(y | u = 1) - H(y | \mathbf{r}, u = 1) \\ &= H(y | u = 1) + \mathbb{E}_{p(y, \mathbf{r}, u)} [\log p(y | \mathbf{r}, u = 1)] \\ &= H(y | u = 1) + \mathbb{E}_{p(y, \mathbf{r}, u)} [\log q_\Omega(y | \mathbf{r}, u = 1)] \\ &\quad + \mathbb{E}_{p(y, \mathbf{r}, u)} [KL(p(\cdot | \mathbf{r}, u = 1) || q_\Omega(\cdot | \mathbf{r}, u = 1))] \\ &\geq H(y | u = 1) + \mathbb{E}_{p(y, \mathbf{r}, u)} [\log q_\Omega(y | \mathbf{r}, u = 1)], \end{aligned}$$

where q_Ω is an *arbitrary* auxiliary posterior distribution that aims to accurately predict the training data label y from the representation \mathbf{r} . Hence, our **Goal 2** for utility preservation can be rewritten as the following *max-max* objective function:

$$\max_f I(y; \mathbf{r} | u = 1) \iff \max_f \max_{\Omega} \mathbb{E}_{p(y, \mathbf{r}, u)} [\log q_\Omega(y | \mathbf{r}, u = 1)] \quad (5)$$

Remark. Equation (5) can be interpreted as a *cooperative game* between the encoder f and q_Ω (e.g., a label predictor) that aims to preserve the utility collaboratively.

Objective function of Inf²Guard against MIAs. By combining Equations (4) and (5), our objective function of learning privacy-preserving representations against MIAs is:

$$\begin{aligned} \max_f \left(\lambda \min_{\Psi} - \mathbb{E}_{p(\mathbf{x}, u)} [\log q_\Psi(u | f(\mathbf{x}))] \right. \\ \left. + (1 - \lambda) \max_{\Omega} \mathbb{E}_{p(\mathbf{x}, y, u)} [\log q_\Omega(y | f(\mathbf{x}), u = 1)] \right), \quad (6) \end{aligned}$$

where $\lambda \in [0, 1]$ tradeoffs privacy and utility. That is, a larger λ indicates a stronger membership privacy protection, while a smaller λ indicates a better utility preservation.

3.1.3 Implementation in practice

In practice, we solve Equation (6) via training three parameterized neural networks (i.e., encoder f , membership protection network g_Ψ associated with the posterior distribution q_Ψ , and utility preservation network h_Ω associated with the posterior distribution q_Ω) using data samples from the underlying data distribution. Specifically, we first collect two datasets D_1 and D_0 from a (larger) dataset, and they include the members and non-members, respectively. Then, D_1 is used for training the utility network h_Ω (i.e., predicting labels for training data D_1) and the encoder f ; and both D_1 and D_0 are used for training the membership protection network g_Ψ (i.e., inferring whether a data sample from D_1/D_0 is a member or not) and the encoder f . With it, we can approximate the expectation terms in Equation (6) and use them to train the neural networks.

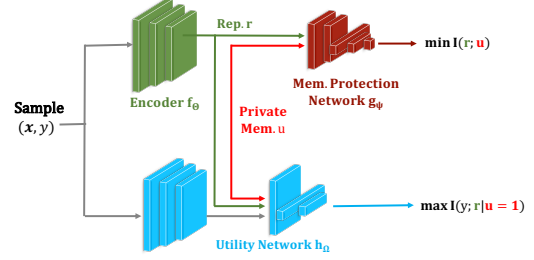


Figure 1: Inf²Guard against MIAs.

Training the membership protection network g_Ψ : We approximate the first expectation w.r.t. q_Ψ as⁷

$$\mathbb{E}_{p(\mathbf{x}, u)} \log q_\Psi(u | f(\mathbf{x})) \approx - \sum_{(\mathbf{x}_j, u_j) \in D_1 \cup D_0} H(u_j, g_\Psi(f(\mathbf{x}_j))),$$

where $H(a, b)$ is the cross-entropy loss between a and b . Take a single data \mathbf{x} with private u for example. The above equation is obtained by: $-H(u, g_\Psi(f(\mathbf{x}))) = \log q_\Psi(f(\mathbf{x}))_u = \log q_\Psi(u | f(\mathbf{x}))$, where $g_\Psi(f(\mathbf{x}))_i$ indicates i -th entry probability, and $q_\Psi(u | f(\mathbf{x}))$ means the probability of inferring \mathbf{x} 's member u . The adversary maximizes this expectation aiming to enhance the membership inference performance.

Training the utility preservation network h_Ω : We approximate the second expectation w.r.t. q_Ω as:

$$\mathbb{E}_{p(\mathbf{x}, y, u)} \log q_\Omega(y | f(\mathbf{x}), u = 1) \approx - \sum_{(\mathbf{x}_j, y_j) \in D_1} H(y_j, h_\Omega(f(\mathbf{x}_j))).$$

We maximize this expectation to enhance the utility.

Training the encoder f : With the updated g_Ψ and h_Ω , the defender performs gradient ascent on Equation (6) to update f , which can learn representations that protect membership privacy and further enhance the utility.

We iteratively train the three networks until reaching pre-defined maximum rounds. Figure 1 illustrates our Inf²Guard against MIAs. Algorithm 1 in Appendix details the training.

Connection with AdvReg [48]. We observe that AdvReg is a special case of Inf²Guard. Specifically, the objective function of AdvReg can be rewritten as:

$$\max_f \left(\lambda \min_{\Psi} \sum_{(\mathbf{x}_j, u_j) \in D_1 \cup D_0} H(u_j, g_\Psi(f(\mathbf{x}_j))) - (1 - \lambda) \sum_{(\mathbf{x}_j, y_j) \in D_1} H(y_j, f(\mathbf{x}_j)) \right),$$

where $f: \mathcal{X} \rightarrow [0, 1]^{|D_1|}$ now outputs a sample's probabilistic confidence score and g_Ψ is a membership inference model aiming to distinguish between members and non-members.

3.2 Inf²Guard against PIAs

Different from MIAs, PIAs leak the training data properties at the *dataset-level*. To align this, instead of using a random sample (\mathbf{x}, y) , we consider a random dataset (\mathbf{X}, \mathbf{y}) in PIAs. Specifically, let $\mathbf{X} = \{\mathbf{x}_i\}$ consist of a set of independent data samples and $\mathbf{y} = \{y_i\}$ the corresponding data labels that are sampled from the underlying data distribution \mathcal{D} ; and \mathbf{X} is associated with a private (dataset) property u .

⁷We omit the sample size $|D_1|, |D_0|$ for description brevity.

3.2.1 MI objectives

Given a dataset $\mathbf{X} \sim \mathcal{D}$ with a property u , the defender learns a dataset representation $\mathbf{R} = f(\mathbf{X})$ that satisfies two goals⁸:

- **Goal 1: Property protection.** \mathbf{R} contains as less information as possible about the private dataset property u . Ideally, when \mathbf{R} does not include information about u (i.e., $\mathbf{R} \perp u$), it is impossible to infer u from \mathbf{R} . Formally, we quantify the property protection using the below MI objective:

$$\min_f I(\mathbf{R}; u). \quad (7)$$

- **Goal 2: Utility preservation.** \mathbf{R} includes as much information as possible about predicting \mathbf{y} . Formally, we quantify the utility preservation using the MI objective as below:

$$\max_f I(\mathbf{y}; \mathbf{R}). \quad (8)$$

3.2.2 Estimating MI via tractable bounds

We estimate the bounds of Equations 7 and 8 as below.

Minimizing the upper bound MI in Equation (7). Following membership protection, **Goal 1** is reformulated as solving the below min-max objective function:

$$\min_f I(\mathbf{R}; u) \iff \min_f \max_{\Psi} \mathbb{E}_{p(\mathbf{R}, u)} [\log q_{\Psi}(u|\mathbf{R})], \quad (9)$$

where $q_{\Psi}(u|\mathbf{R})$ is an arbitrary posterior distribution.

Remark. Similarly, Equation (9) can be interpreted as an *adversarial game* between a property inference adversary q_{Ψ} who aims to infer u from the dataset representations \mathbf{R} and the encoder f who aims to protect u from being inferred.

Maximizing the lower bound MI in Equations (8). Similarly, we adopt the MI estimator [49] to estimate the lower bound MI in our **Goal 2**, which can be rewritten as the following max-max objective function:

$$\max_f I(\mathbf{y}; \mathbf{R}) \iff \max_f \max_{\Omega} \mathbb{E}_{p(\mathbf{y}, \mathbf{R})} [\log q_{\Omega}(\mathbf{y}|\mathbf{R})], \quad (10)$$

where q_{Ω} is an *arbitrary* posterior distribution that aims to predict each label $y \in \mathbf{y}$ from the data representation $\mathbf{r} \in \mathbf{R}$.

Remark. Equation (10) can be interpreted as a *cooperative game* between f and q_{Ω} to preserve the utility collaboratively.

Objective function of Inf^2Guard against PIAs. By combining Equations (9) and (10), our objective function of learning privacy-preserving representations against PIAs is:

$$\max_f \left(\lambda \min_{\Psi} \mathbb{E}_{p(\mathbf{X}, u)} [\log q_{\Psi}(u|f(\mathbf{X}))] + (1 - \lambda) \max_{\Omega} \mathbb{E}_{p(\mathbf{X}, \mathbf{y})} [\log q_{\Omega}(\mathbf{y}|f(\mathbf{X}))] \right), \quad (11)$$

where $\lambda \in [0, 1]$ tradeoffs between privacy and utility. That is, a larger/smaller λ indicates less/more dataset property can be inferred through the learnt dataset representation.

⁸For notation simplicity, we use the same f to indicate the encoder. Similar for subsequent notations such as g_{Ψ} , h_{Ω} , q_{Ω} , h_{Ω} , etc.

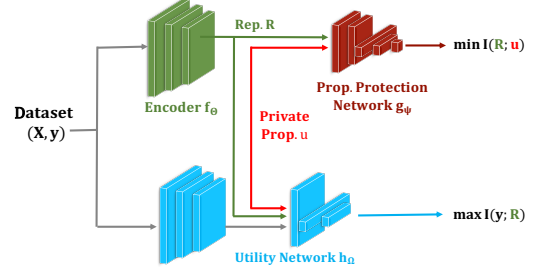


Figure 2: Inf^2Guard against PIAs.

3.2.3 Implementation in practice

Equation (11) is solved via three parameterized neural networks (i.e., the encoder f_{Θ} , the property protection network g_{Ψ} associated with q_{Ψ} , and the utility preservation network h_{Ω} associated with q_{Ω}) using a set of *datasets* sampled from a data distribution. Specifically, we first collect a large reference dataset D_r . Then, we randomly generate a set of small datasets $\{D_j = (\mathbf{X}_j, \mathbf{y}_j)\}_j$ from D_r . We denote the dataset property value for each D_j as u_j . With it, we can approximate the expectation terms in Equation (11).

Training the property inference network g_{Ψ} : We approximate the first expectation w.r.t. q_{Ψ} as

$$\mathbb{E}_{p(\mathbf{X}, u)} \log q_{\Psi}(u|f(\mathbf{X})) \approx - \sum_{\{\mathbf{X}_j \in D_j\}} H(u_j, g_{\Psi}(f(\mathbf{X}_j))), \quad (12)$$

where $f(\mathbf{X}_j)$ is the aggregated representation of a dataset \mathbf{X}_j , i.e., $f(\mathbf{X}_j) = \text{Agg}(\{f(\mathbf{x})\}_{\mathbf{x} \in \mathbf{X}_j})$. We will discuss the aggregator $\text{Agg}(\cdot)$ in Section 5.2.2. The adversary maximizes this expectation to enhance the property inference performance.

Training the utility preservation network h_{Ω} : Similarly, we approximate the second expectation w.r.t. q_{Ω} as:

$$\mathbb{E}_{p(\mathbf{X}, \mathbf{y})} \log q_{\Omega}(\mathbf{y}|f(\mathbf{X})) \approx - \sum_{\{D_j\}} \sum_{\{\mathbf{x}_i, \mathbf{y}_i \in D_j\}} H(\mathbf{y}_i, h_{\Omega}(f(\mathbf{x}_i))), \quad (13)$$

where we maximize this expectation to enhance the utility.

Training the encoder f : The defender then performs gradient ascent on Equation (11) to update f , which mitigates the PIA and further enhances the utility.

We iteratively train the three networks until reaching maximum rounds. Figure 2 illustrates our Inf^2Guard against PIAs. Algorithm 2 in Appendix details the training process.

3.3 Inf^2Guard against DRAs

Different from MIAs and PIAs, DRAs aim to *directly* recover the training data from the learnt representations. A recent defense [65] shows perturbing the latent representations can somewhat protect the data from being reconstructed. However, this defense is broken by an advanced attack [9]. One key reason is the defense perturbs representations in a *deterministic* fashion for already *trained* models. We address the issues and propose an information-theoretic defense to learn

randomized representations against the DRAs in an end-to-end *learning* fashion. Our core idea is to learn a *deterministic* encoder and a *randomized* perturbator that ensures learning the perturbed representation in a controllable manner.

3.3.1 MI objectives

Given a data sample $\mathbf{x} \sim \mathcal{D}$ with a label y , the defender learns a representation $\mathbf{r} = f(\mathbf{x})$ such that when \mathbf{r} is perturbed by certain perturbation (denoted as $\boldsymbol{\delta}$), the shared perturbed representation $\mathbf{r} + \boldsymbol{\delta}$ cannot be used to well recover \mathbf{x} , but is effective for predicting y , from the information-theoretic perspective. Then we aim to achieve the following two goals:

- **Goal 1: Data reconstruction protection.** $\mathbf{r} + \boldsymbol{\delta}$ contains as less information as possible about \mathbf{x} . Moreover, the perturbation $\boldsymbol{\delta}$ should be effective enough. Hence, we require $\boldsymbol{\delta}$ can cover all directions of \mathbf{x} , and force the entropy of $\boldsymbol{\delta}$ to be as large as possible. Formally, we quantify the data reconstruction protection using the below MI objective:

$$\min_{f, p(\boldsymbol{\delta}) \sim \mathcal{P}} I(\mathbf{r} + \boldsymbol{\delta}; \mathbf{x}) - H(\boldsymbol{\delta}), \quad (14)$$

- **Goal 2: Utility preservation.** To ensure \mathbf{r} be useful, it should be effective for predicting the label y . Further, as we will share the perturbed representation $\mathbf{r} + \boldsymbol{\delta}$, it should be also effective for predicting y . Formally, we quantify the utility preservation using the MI objective as follows:

$$\max_{f, p(\boldsymbol{\delta}) \sim \mathcal{P}} I(\mathbf{r} + \boldsymbol{\delta}; y) + I(\mathbf{r}; y), \quad (15)$$

3.3.2 Estimating MI via tractable bounds

Minimizing the upper bound MI in Equation (14). Similarly, we adapt the variational upper bound in [16]. Our **Goal 1** for data reconstruction protection can be reformulated as the below *min-max* objective function:

$$\begin{aligned} & \min_{f, p(\boldsymbol{\delta}) \sim \mathcal{P}} I(\mathbf{r} + \boldsymbol{\delta}; \mathbf{x}) - \alpha H(\boldsymbol{\delta}) \\ \iff & \min_{f, p(\boldsymbol{\delta}) \sim \mathcal{P}} \left(\max_{\Psi} \mathbb{E}_{p(\mathbf{x}, \boldsymbol{\delta}, \mathbf{x})} [\log q_{\Psi}(\mathbf{x} | \mathbf{r} + \boldsymbol{\delta})] - \alpha H(\boldsymbol{\delta}) \right). \end{aligned} \quad (16)$$

Remark. Equation (16) can be interpreted as an *adversarial game* between an adversary q_{Ψ} (i.e., data reconstructor) who aims to infer \mathbf{x} from $\mathbf{r} + \boldsymbol{\delta}$; and the encoder f who aims to protect \mathbf{x} from being inferred via carefully perturbing \mathbf{r} .

Maximizing the lower bound MI in Equation (15). Based on [53], we can produce a lower bound on the MI $I(\mathbf{r}; y)$ due to the non-negativity of the KL-divergence:

$$\begin{aligned} I(\mathbf{r}; y) &= \mathbb{E}_{p(y, \mathbf{r})} [\log q_{\Omega}(y | \mathbf{r}) / p(y)] + \mathbb{E}_{p(\mathbf{r})} [KL(p(y | \mathbf{r}) || q_{\Omega}(y | \mathbf{r}))] \\ &\geq \mathbb{E}_{p(y, \mathbf{r})} [\log q_{\Omega}(y | \mathbf{r})] + H(y), \end{aligned} \quad (17)$$

where q_{Ω} is an *arbitrary* posterior distribution that predicts the label y from \mathbf{r} and the entropy $H(y)$ is a constant.

We have a similar form for the MI $I(\mathbf{r} + \boldsymbol{\delta}; y)$ as below

$$I(\mathbf{r} + \boldsymbol{\delta}; y) \geq \max_{p(\boldsymbol{\delta}) \sim \mathcal{P}} \mathbb{E}_{p(y, \mathbf{r}, \boldsymbol{\delta})} [\log q_{\Omega}(y | \mathbf{r} + \boldsymbol{\delta})] + H(y), \quad (18)$$

where we use the same q_{Ω} to predict the label y from the perturbed representation $\mathbf{r} + \boldsymbol{\delta}$.

Then, our **Goal 2** for utility preservation can be rewritten as the following max-max objective function:

$$\begin{aligned} & \max_{f, p(\boldsymbol{\delta}) \sim \mathcal{P}} I(\mathbf{r} + \boldsymbol{\delta}; y) + I(\mathbf{r}; y) \\ \iff & \max_{f, \Omega} \left(\max_{p(\boldsymbol{\delta}) \sim \mathcal{P}} \mathbb{E}_{p(y, \mathbf{r}, \boldsymbol{\delta})} [\log q_{\Omega}(y | \mathbf{r} + \boldsymbol{\delta})] + \mathbb{E}_{p(y, \mathbf{r})} [\log q_{\Omega}(y | \mathbf{r})] \right). \end{aligned} \quad (19)$$

Remark. Equation (19) can be interpreted as a *cooperative game* between the encoder f and the label prediction network q_{Ω} , who aim to preserve the utility collaboratively.

Objective function of Inf²Guard against DRAs. By combining Equations (16)-(19), our objective function of learning privacy-preserving representations against DRAs is:

$$\begin{aligned} & \max_{f, p(\boldsymbol{\delta}) \sim \mathcal{P}} \left(\lambda \left(\min_{\Psi} \mathbb{E}_{p(\mathbf{x}, \boldsymbol{\delta})} [\log q_{\Psi}(\mathbf{x} | f(\mathbf{x}) + \boldsymbol{\delta})] + \alpha H(\boldsymbol{\delta}) \right) \right. \\ & \left. + (1 - \lambda) \left(\max_{\Omega} \mathbb{E}_{p(\mathbf{x}, \boldsymbol{\delta}, y)} [\log q_{\Omega}(y | f(\mathbf{x}) + \boldsymbol{\delta})] + \mathbb{E}_{p(\mathbf{x}, y)} [\log q_{\Omega}(y | f(\mathbf{x}))] \right) \right), \end{aligned} \quad (20)$$

where $\lambda \in [0, 1]$ tradeoffs privacy and utility. A larger λ implies less data features can be inferred through the perturbed representation, while a smaller λ implies the shared perturbed representation is easier for predicting the label.

3.3.3 Parameterizing perturbation distributions

The key of our defense lies in defining the perturbation distribution $p(\boldsymbol{\delta})$ in Equation (20). Directly specifying the optimal perturbation distribution is challenging. Motivated by variational inference [39], we propose to parameterize $p(\boldsymbol{\delta})$ with trainable parameters, e.g., Φ . Then the optimization problem w.r.t. the perturbation $\boldsymbol{\delta}$ can be converted to be w.r.t. the parameters Φ , which can be solved via back-propagation.

A natural way to model the perturbation around a representation is using a distribution with an explicit density function. Here we adopt the method in [39] by transforming $\boldsymbol{\delta}$ such that the reparameterization trick can be used in training. For instance, when considering $p_{\Phi}(\boldsymbol{\delta})$ as a Gaussian distribution $\mathcal{N}(\boldsymbol{\mu}, \boldsymbol{\sigma}^2)$, we can reparameterize $\boldsymbol{\delta}$ (with a scale ε) as:

$$\boldsymbol{\delta} = \varepsilon \cdot \tanh(\mathbf{u}), \quad \mathbf{u} \sim \mathcal{N}(\boldsymbol{\mu}, \text{diag}(\boldsymbol{\sigma}^2)), \quad (21)$$

That is, it first samples \mathbf{u} from a diagonal Gaussian with a mean vector $\boldsymbol{\mu}$ and standard deviation vector $\boldsymbol{\sigma}$, and $\boldsymbol{\delta}$ is obtained by compressing \mathbf{u} to be $[-1, 1]$ via the $\tanh(\cdot)$ function and multiplying ε . $\Phi = (\boldsymbol{\mu}, \boldsymbol{\sigma})$ are the parameters to be learnt.

3.3.4 Implementation in practice

We train three neural networks (i.e., the encoder f , reconstruction protection network g_{Ψ} , and utility preservation network h_{Ω}) using data samples from certain data distribution. Suppose we are given a set of data samples $D = \{\mathbf{x}_j, y_j\}$.

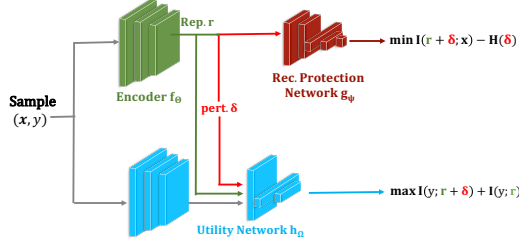


Figure 3: Inf^2Guard against DRAs.

Learning the data reconstruction network g_Ψ : As \mathbf{x} and its representation \mathbf{r} are often high-dimensional, the previous MI estimators are inappropriate in this setting. To address it, we use the *Jensen-Shannon* divergence (JSD) [32] specially for high-dimensional MI estimation. Assume we have updated Φ . We can approximate the expectation w.r.t. g_Ψ as

$$\begin{aligned} \mathbb{E}_{p(\mathbf{x}), p_\Phi(\delta)} \log q_\Psi(\mathbf{x}|f(\mathbf{x}) + \delta) &= I_{\Theta, \Psi}^{(\text{JSD})}(\mathbf{x}; f_\Theta(\mathbf{x}) + \delta) \\ &\approx \sum_{\mathbf{x}_j \in D, \delta_j \sim p_\Phi(\delta)} [-\text{sp}(-h_\Psi(\mathbf{x}_j, f_\Theta(\mathbf{x}_j) + \delta_j))] \\ &\quad - \sum_{(\mathbf{x}_j, \mathbf{x}'_j) \in D, \delta_j \sim p_\Phi(\delta)} [\text{sp}(h_\Psi(\mathbf{x}'_j, f_\Theta(\mathbf{x}_j) + \delta_j))], \end{aligned} \quad (22)$$

where \mathbf{x}'_j is an independent and random sample from the same distribution as \mathbf{x}_j , and $\text{sp}(z) = \log(1 + \exp(z))$ is the softplus function. We maximize $I_{\Theta, \Psi}^{(\text{JSD})}$ to update g_Ψ .

Learning the utility preservation network h_Ω : We first estimate the below expectation:

$$\mathbb{E}_{p(\mathbf{x}, y), p_\Phi(\delta)} \log q_\Omega(y|f(\mathbf{x}) + \delta) \approx - \sum_{(\mathbf{x}_j, y_j) \in D, \delta_j \sim p_\Phi(\delta)} H(y_j, h_\Omega(f(\mathbf{x}_j) + \delta_j)). \quad (23)$$

Similarly, we can approximate the third expectation as:

$$\mathbb{E}_{p(\mathbf{x}, y)} \log q_\Omega(y|f(\mathbf{x})) \approx - \sum_{(\mathbf{x}_j, y_j) \in D} H(y_j, h_\Omega(f(\mathbf{x}_j))). \quad (24)$$

We minimize the two cross entropy losses to update h_Ω .

Updating the distribution parameter Φ : Due to the reparameterization trick, the gradient can be back-propagated from each δ_j to the parameters Φ . For simplicity, we do not consider the JSD term in Equation (22) due to its complexity. Then we have the terms relevant to Φ as below:

$$\mathbb{E}_{\mathbf{z} \sim \mathcal{N}(0, 1), (\mathbf{x}_j, y_j)} H(y_j, h_\Omega(f(\mathbf{x}_j) + \varepsilon \cdot \tanh(\boldsymbol{\mu} + \boldsymbol{\sigma}\mathbf{z}))) - \beta \cdot H(\varepsilon \cdot \tanh(\boldsymbol{\mu} + \boldsymbol{\sigma}\mathbf{z})), \quad (25)$$

where $\beta = \lambda\alpha/(1 - \lambda)$. The first term is the cross entropy loss, while the second term is the entropy. The gradient w.r.t. Φ in each term can be calculated. In practice, we approximate the expectation on \mathbf{z} with (e.g., 5) Monte Carlo samples, and perform *stochastic gradient descent* to update Φ . Details on updating Φ are in Algorithm 3. With Φ , we use it to generate δ and add it to \mathbf{r} to produce the perturbed representation.

Learning the encoder f . Finally, after updating g_Ψ , h_Ω , and Φ , we can perform gradient ascent to update f .

We iteratively train the networks until reaching a predefined maximum round. Figure 3 illustrates Inf^2Guard against DRAs. Algorithm 4 in Appendix details the training process.

4 Theoretical Results

We mainly show the guaranteed privacy leakage under Inf^2Guard , with proofs in Appendix A. We also derive an inherent utility-privacy tradeoff of Inf^2Guard , which requires a binary classification task, and binary-valued dataset property in PIAs. Details and proofs are deferred to Appendix B.

Guaranteed privacy leakage of MIAs: Let \mathcal{A}_{MIA} be the set of all MIAs $\mathcal{A}_{MIA} = \{A_{MIA} : \mathcal{Z} \rightarrow u \in \{0, 1\}\}$ that have access to the representations \mathbf{r} by querying f with data \mathbf{x} from the distribution \mathcal{D} . The MIA accuracy is bounded as below:

Theorem 1. *Let f be the learnt encoder by Equation (6) over a data distribution $\mathcal{D} \subset \mathcal{X}$. For a random data sample $\mathbf{x} \sim \mathcal{D}$ with the learnt representation $\mathbf{r} = f(\mathbf{x})$ and membership u , we have $\Pr(A_{MIA}(\mathbf{r}) = u) \leq 1 - \frac{H(u|\mathbf{r})}{2 \log_2(6/H(u|\mathbf{r}))}, \forall A_{MIA} \in \mathcal{A}_{MIA}$.*

Remark. Theorem 1 shows if $H(u|\mathbf{r})$ is larger, the bounded MIA accuracy is smaller. Note $H(u|\mathbf{r}) = H(u) - I(u; \mathbf{r})$ and $H(u)$ is a constant. Achieving a large $H(u|\mathbf{r})$ implies obtaining a small $I(u; \mathbf{r})$, which is our **Goal 1** in Equation (1) does. In practice, once the encoder f is learnt on a dataset from \mathcal{D} , $I(u; \mathbf{r})$ can be estimated, then the bounded MIA accuracy can be calculated. A better encoder f or/and better MI estimator of $I(u; \mathbf{r})$ can yield a smaller MIA performance.

Guaranteed privacy leakage of PIAs: Let \mathcal{A}_{PIA} be the set of all PIAs that have access to the representations \mathbf{R} of a dataset $\mathbf{X} = \{\mathbf{x}_i\}$ sampled from the data distribution \mathcal{D} , i.e., $\mathcal{A}_{PIA} = \{A_{PIA} : \mathcal{Z} \rightarrow u \in \{0, 1\}\}$. The PIA accuracy is bounded as:

Theorem 2. *Let f be the learnt encoder by Equation (11) over a data distribution \mathcal{D} . For a random dataset $\mathbf{X} \sim \mathcal{D}$ with the learnt representation $\mathbf{R} = f(\mathbf{X})$ and dataset property u , we have $\Pr(A_{PIA}(\mathbf{R}) = u) \leq 1 - \frac{H(u|\mathbf{R})}{2 \log_2(6/H(u|\mathbf{R}))}, \forall A_{PIA} \in \mathcal{A}_{PIA}$.*

Remark. Theorem 2 shows when $H(u|\mathbf{R})$ is larger, the PIA accuracy is smaller, i.e., less dataset property is leaked. Also, a large $H(u|\mathbf{R})$ indicates a small $I(u; \mathbf{R})$ —This is exactly our **Goal 1** in Equation (7) aims to achieve.

Guaranteed privacy leakage of DRAs: Let \mathcal{A}_{DRA} be the set of all DRAs that have access to the perturbed data representations, i.e., $\mathcal{A}_{DRA} = \{A_{DRA} : \mathbf{r} + \delta \in \mathcal{Z} \times \mathcal{P} \rightarrow \mathbf{x} \in \mathcal{X}\}$. An ℓ_p -norm ball centered at a point \mathbf{v} with a radius ρ is denoted as $\mathcal{B}_p(\mathbf{v}, \rho)$, i.e., $\mathcal{B}_p(\mathbf{v}, \rho) = \{\mathbf{v}' : \|\mathbf{v}' - \mathbf{v}\|_p \leq \rho\}$. For a space \mathcal{S} , we denote its boundary as $\partial\mathcal{S}$, whose volume is denoted as $\text{Vol}(\partial\mathcal{S})$. Then the reconstruction error (in terms of ℓ_p norm difference) incurred by any DRA is bounded as below:

Theorem 3. *Let f be the encoder learnt by Equation (20) over a data distribution $\mathcal{D} \subset \mathcal{X}$ and δ be the perturbation for a random sample $\mathbf{x} \sim \mathcal{X}$. Then, $\Pr(\|A_{DRA}(\mathbf{r} + \delta) - \mathbf{x}\|_p \geq \eta) \geq 1 - \frac{I(\mathbf{x}; \mathbf{r} + \delta) + \log 2}{\log \text{Vol}(\partial\mathcal{X}) - \log \text{Vol}(\partial\mathcal{X}(\eta))}, \forall A_{DRA} \in \mathcal{A}_{DRA}$, where $\text{Vol}(\partial\mathcal{X}(\eta)) = \max_{\mathbf{x} \in \mathcal{X}} \text{Vol}(\partial\mathcal{B}_p(\mathbf{x}, \eta) \cap \mathcal{X})$.*

Remark. Theorem 3 shows a lower bound error achieved by the strongest DRA. Given an η , when $I(\mathbf{x}; \mathbf{r} + \delta)$ is smaller, the lower bound data reconstruction error is larger, meaning the privacy of the data itself is better protected. Moreover, minimizing $I(\mathbf{x}; \mathbf{r} + \delta)$ is exactly our **Goal 1** in Equation (14).

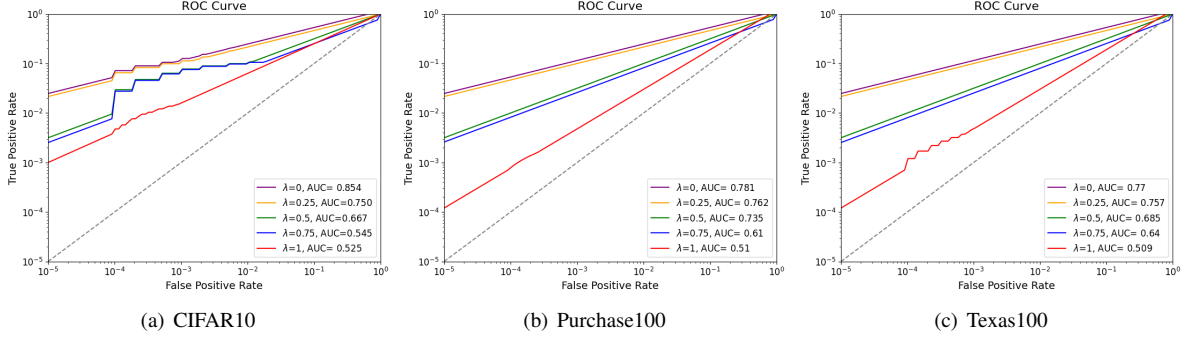


Figure 4: TPR vs FPR of Inf^2Guard against LiRA on different λ 's.

5 Evaluations

In this section, we will evaluate Inf^2Guard against the MIAs, PIAs, and DRAs on benchmark datasets. Inf^2Guard involves training the encoder, the privacy protection network, and the utility preservation network. The detailed dataset description and architectures of the networks are given in Appendix C.

5.1 Defense Results on MIAs

5.1.1 Experimental setup

Datasets: Following existing works [38, 48], we use the CIFAR10 [40], Purchase100 [48], and Texas100 [61] datasets, to evaluate Inf^2Guard against MIAs.

Defense/attack training and testing: The training sets and test sets are listed in Table 9 in Appendix C.2. For instance, in CIFAR10, we use 50K samples in total and split it into two halves, where 25K samples are used as the *utility training set* ("members") and the other 25K samples as the *utility test set* ("non-members"). We select 80% of the members and non-members as the *attack training set* and the remaining members and non-members as the *attack test set*.

- **Defense training:** We use the utility training set and attack training set to train the encoder, utility preservation network, and membership protection network simultaneously. Then, the learnt encoder is frozen and published as an API.
- **Attack training:** To mimic the strongest possible MIA, we let the attacker know the exact membership protection network and attack training set used in defense training. Specifically, s/he feeds the attack training set to the learnt encoder to get the data representations and trains the MIA classifier (same as the membership protection network) on these representations to maximally infer the membership.
- **Defense and attack testing:** We use the utility test set to obtain the utility (i.e., test accuracy) via querying the trained encoder and utility network. Moreover, we use the attack test set to obtain the MIA performance.

Privacy metric: We measure the MIA performance via both the MIA accuracy and the true positive rate (TPR) vs. false positive rate (FPR), suggested by the SOTA LiRA MIA [13].

Table 1: Inf^2Guard results against MIAs on the three dataset. $\lambda = 0$ means no privacy protection, while $\lambda = 1$ means no utility preservation. Random guessing MIA accuracy is 50%.

CIFAR10			Purchase100			Texas100		
λ	Utility	MIA Acc	λ	Utility	MIA Acc	λ	Utility	MIA Acc
0	78.9%	70.1%	0	81.7%	68.4%	0	49.9%	70.2%
0.25	78.2%	55.9%	0.25	80.9%	60%	0.25	49.1%	61%
0.5	78%	53.5%	0.5	80%	51%	0.5	47%	53%
0.75	77.2%	51.1%	0.75	78%	50%	0.75	46%	50%
1	20%	50%	1	20%	50%	1	2%	50%

Specifically, the MIA accuracy is obtained by querying the trained encoder and trained MIA classifier with the attack test set. Moreover, we treat the representations and membership network learnt by Inf^2Guard as the input data and target model for LiRA. We then train 16 *white-box* shadow models (i.e., assume LiRA uses the exact membership network in Inf^2Guard) on the data representations of the utility training set, and report the TPR vs. FPR on the attack test set.

5.1.2 Experimental results

Utility-privacy results: According to Equation (6), $\lambda = 0$ indicates no privacy protection. Increasing λ 's value enhances Inf^2Guard 's resilience against MIAs. $\lambda = 1$ means the maximum privacy protection without preserving utility. Table 1 shows the utility-MIA Accuracy results of Inf^2Guard . We have the following observations: 1) The MIA accuracy is the largest when $\lambda = 0$, implying leaking the most membership privacy by MIAs. 2) When only protecting privacy ($\lambda = 1$), the MIA accuracy reaches to the optimal random guessing, but the utility is the lowest. 3) When $0 < \lambda < 1$, Inf^2Guard obtains reasonable utility and MIA accuracy. Especially, when $\lambda = 0.75$, the utility loss is marginal (i.e., $< 4\%$), while the MIA accuracy is (close to) random guessing. The results show the learnt privacy-preserving encoder/representations are effective against MIAs, and maintain utility as well.

Further, Figure 4 shows the TPR vs FPR of Inf^2Guard against LiRA. Similarly, we observe that the TPR at low FPRs is relatively large (strong membership inference) in case of no privacy protection, but it can be largely reduced by increasing λ . This implies that Inf^2Guard indeed learns the representations that can defend against LiRA to some extent.

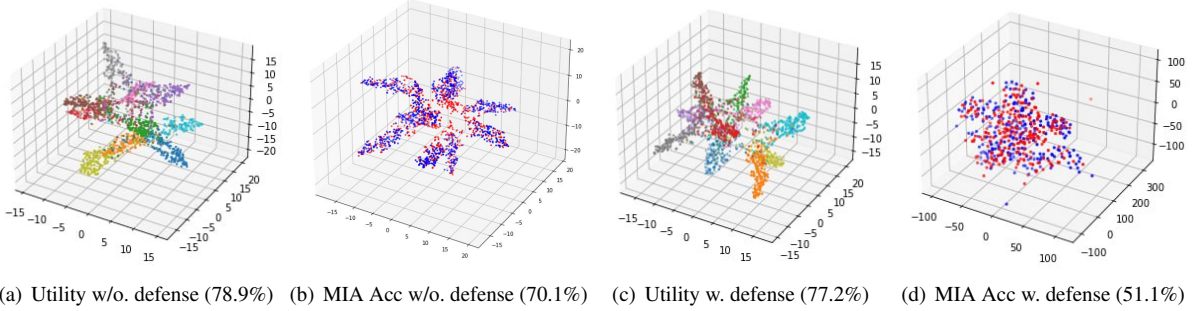


Figure 5: Inf^2Guard against MIAs: 3D t-SNE embeddings results on the learnt representation of on CIFAR10.

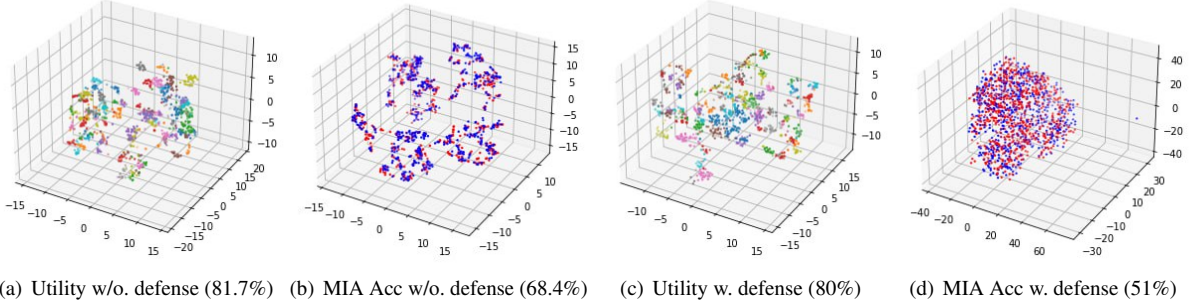


Figure 6: Inf^2Guard against MIAs: 3D t-SNE embeddings results on the learnt representation on Purchase100.

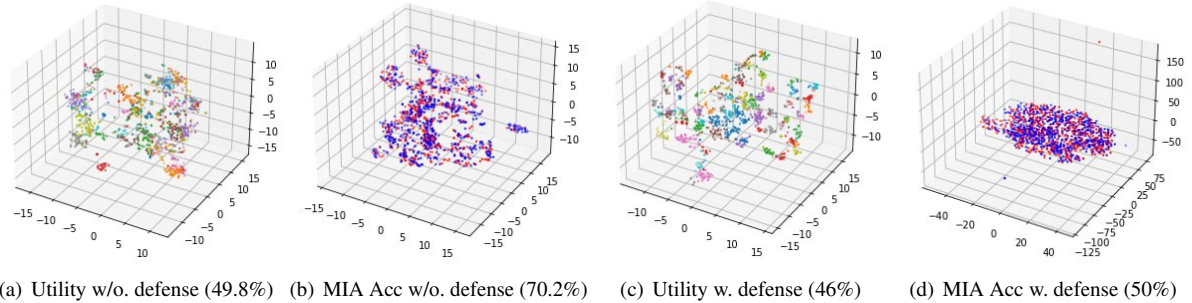


Figure 7: Inf^2Guard against MIAs: 3D t-SNE embeddings results on the learnt representation on Texas100.

Visualizing the learnt representations: To better understand the learnt representations by Inf^2Guard , we adopt the t-SNE algorithm [67] to visualize the low-dimensional embeddings of them. λ is chosen in Table 1 that achieves the best utility-privacy tradeoff. We also compare with the case without privacy protection. Figures 5-7 show the 3D t-SNE embeddings, where each color corresponds to a label in the learning task or (non)member in the privacy task, and each point is a data sample. We can observe the t-SNE embeddings of the learnt representations without privacy protection for members and non-members are separated to some extent, meaning the membership can be inferred via the learnt MIA classifier. On the contrary, the t-SNE embeddings of the learnt representations by our Inf^2Guard for members and non-members are mixed—hence making it difficult for the (best) MIA classifier to infer the membership from these learnt representations.

Comparing with the existing defenses against MIAs: All empirical defenses are broken by stronger attacks [17, 62], except adversarial training-based AdvReg [48] (a special case

Table 2: Comparing Inf^2Guard with existing defenses against MIAs on the three datasets. DP methods are under the same/close defense performance as Inf^2Guard .

Defense	CIFAR10		Purchase100		Texas100	
	Utility	MIA Acc	Utility	MIA Acc	Utility	MIA Acc
DP-SGD	48%	51%	40%	52%	11%	51%
DP-enc	45%	51%	32%	51%	10%	50%
AdvReg	75%	53%	75%	51%	44%	52%
NeuGuard	74%	56%	77%	53%	43%	52%
Inf^2Guard	77%	51%	80%	51%	46%	50%

of Inf^2Guard). NeuGuard [74] is a recent empirical defense and shows better performance than, e.g., [38, 60]. Differential privacy is the only defense with privacy guarantees. We propose to use two DP variants, i.e., DP-SGD [3] and DP-encoder (details in Appendix C.2). The comparison results of these defenses are shown in Table 2 (more DP results in Table 16 in Appendix C.4) and Figure 8. From Table 2, we observe DP methods have bad utility when ensuring the same level defense performance (w.r.t. MIA accuracy) as Inf^2Guard . AdvReg and NeuGuard also perform worse than Inf^2Guard .

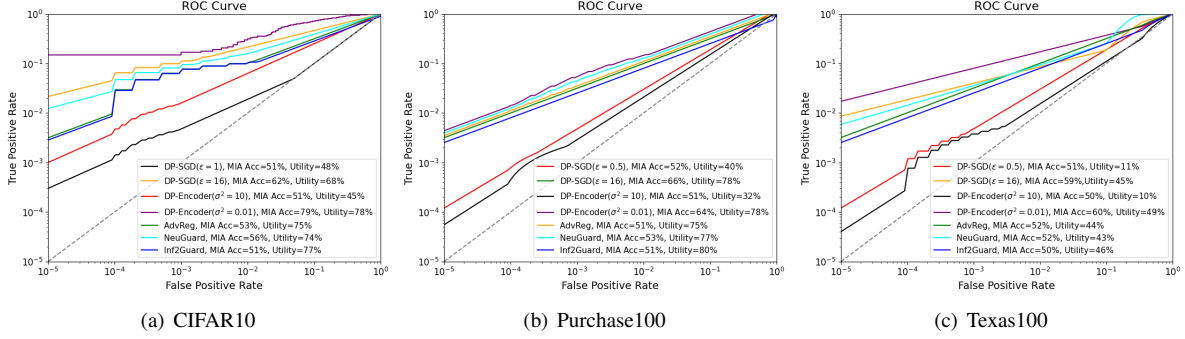


Figure 8: Comparing Inf^2Guard ($\lambda = 0.75$) with the existing defenses against LiRA.

Figure 8 shows the TPR vs. FPR of these defenses against LiRA under the results in Table 2. For DP methods, we also plot the TPR vs FPR when their utility is close to Inf^2Guard . With an MIA accuracy close to random guessing (but low utility), we see DP methods have the smallest TPR at a given low FPR. This means DP methods can most reduce the attack effectiveness of LiRA, which is also verified in [13]. However, if DP methods have a close utility as Inf^2Guard , their TPRs are much higher than Inf^2Guard 's at a low FPR. Besides, Inf^2Guard has smaller TPRs than AdvReg and NeuGuard.

Overhead comparison: All MIA defenses train a task classifier. AdvReg trains a task classifier and membership inference network. NeuGuard trains a task classifier with two regularizations. DP-SGD trains the task classifier on noisy models, while DP-encoder normally trains the encoder first and then trains the utility network on (Gaussian) noisy representations. In the experiments, we define the task classifier of the compared defenses as the concatenation of our encoder and utility network. In our platform (NVIDIA GeForce RTX 3070 Ti), it took Inf^2Guard (72,7,6), AdvReg (66,6,6), NeuGuard (62,5,5), DP-SGD (60,4,3) and DP-encoder (59,4,3) seconds to run each iteration on the three datasets, respectively⁹.

5.2 Defense Results on PIAs

5.2.1 Experimental setup

Datasets: Following recent works [14, 66], we use three datasets (Census [66], RSNA [66], and CelebA [43]) and treat the female ratio as the private dataset property.

Defense/attack training and testing: We first predefine a (different) female ratio set in each dataset. For each female ratio, we generate a number of subsets from the training set and test set with different subset sizes. The generated training/test subsets and all data samples in these subsets are treated as the attack training/test set and the utility training/test set, respectively. More details are in Table 10 in Appendix C.2.

- **Defense training:** We use the utility training set and attack training set to train the encoder, utility preservation network, and property protection network simultaneously. Then, the learnt encoder is frozen and published as an API.

⁹We have similar conclusions on defending against the other two attacks.

Table 3: Inf^2Guard results against PIAs with a mean-aggregation. $\lambda = 0$ means no privacy protection, while $\lambda = 1$ means no utility preservation. Random guessing PIA accuracy on the three datasets are 25%, 14.3%, and 9.1%, respectively.

Census			RSNA			CelebA		
λ	Utility	PIA Acc	λ	Utility	PIA Acc	λ	Utility	PIA Acc
0	85%	68%	0	83%	52%	0	91%	50%
0.25	80%	61%	0.25	82%	25%	0.25	91%	28%
0.5	78%	52%	0.5	82%	24%	0.5	91%	17%
0.75	76%	34%	0.75	80%	19%	0.75	89%	11%
1	45%	26%	1	50%	15%	1	53%	10%

- **Attack training:** We mimic the strongest possible PIA, where the attacker knows the exact property protection network, the aggregator, and attack training set used in defense training. Specifically, s/he feeds each subset in the attack training set to the learn encoder to get the subset representation, applies the aggregator to obtained the aggregated representation, and trains the PIA classifier (same as the property protection network) on these aggregated representations to maximally infer the private female ratio.
- **Defense/attack testing:** We utilize the utility test set to obtain the utility via querying the trained encoder and utility network, and the attack test set to obtain the PIA accuracy via querying the trained encoder and trained PIA classifier.

5.2.2 Experimental results

Utility-privacy results: Table 3 shows the utility-privacy results of Inf^2Guard , where the encoder uses a mean-aggregator (i.e., average the representations of a subset of data. Note different subsets have different sizes). We have similar observations as in defending against MIAs: 1) The PIA accuracy can be as large as 68% without privacy protection ($\lambda = 0$ in Equation (11)), implying the PIA is effective; 2) When focusing on protecting privacy ($\lambda = 1$), the PIA performance can be largely reduced. However, the utility is also significantly decreased, e.g., from 85% to 45%. 3) Utility and privacy show a tradeoff w.r.t. $0 < \lambda < 1$. In most of the cases, the best tradeoff is obtained when $\lambda = 0.75$. Again, the results show the learnt privacy-preserving encoder/representations are effective against PIAs, and also maintain utility.

Table 4: Inf²Guard results against PIAs with a **max**-aggregation. Random guessing PIA accuracy on the three datasets are 25%, 14.3%, and 9.1%, respectively.

Census			RSNA			CelebA		
λ	Utility	PIA Acc	λ	Utility	PIA Acc	λ	Utility	PIA Acc
0	85%	65%	0	83%	52%	0	91%	50%
0.25	83%	51%	0.25	82%	24%	0.25	91%	25%
0.5	79%	49%	0.5	82%	24%	0.5	91%	15%
0.75	77%	37%	0.75	81%	21%	0.75	88%	15%
1	47%	30%	1	50%	16%	1	53%	9%

Table 5: Comparing Inf²Guard with DP against PIAs.

Defense	Census		RSNA		CelebA	
	Utility	PIA Acc	Utility	PIA Acc	Utility	PIA Acc
DP-encoder	52%	34%	57%	19%	66%	11%
Inf ² Guard	76%	34%	80%	19%	89%	11%

Visualizing the learnt representations: Figures 12-14 in Appendix C.4 show the 3D t-SNE embeddings of the learnt representations with $\lambda = 0, 0.75$. Similarly, we observe the t-SNE embeddings of the aggregated representations without privacy protection can be separated to a large extent, while those with privacy protection by Inf²Guard are mixed. This again verifies it is difficult for the (best) PIA to infer the private female ratio from the representations learnt by Inf²Guard.

Impact of the aggregator used by the encoder: In this experiment, we test the impact of the aggregator and choose a max-aggregator for evaluation, where we select the element-wise maximum value of the representations of each subset of data. Table 4 shows the results. We have similar conclusions as those with the mean-aggregator. In addition, Inf²Guard with the max-aggregator has slightly worse utility-privacy tradeoff, compared with the mean-aggregator. A possible reason could be the mean-aggregator uses more information of the subset representations than the max-aggregator.

Comparing with the DP-based defense: There exists no effective defense against PIAs, and [66] shows DP-SGD [3] does not work well. Here, we propose to use a DP variant called DP-encoder, similar to that against MIAs. More details about DP-encoder are in Appendix C.2. The compared results are shown in Table 5. We can see that, with the same level privacy protection as Inf²Guard, DP has much worse utility.

5.3 Defense Results on DRAs

5.3.1 Experimental setup

Datasets: We select two image datasets: CIFAR10 [40] and CIFAR100 [40], and one human activity recognition dataset Activity [54] to evaluate Inf²Guard against DRAs.

Defense/attack training and testing: Table 11 in Appendix shows the statistics of the utility/attack training and test sets.

- **Defense training:** We use the training set to train the encoder, utility preservation network, reconstruction protection network, and update the perturbation distribution parameters, simultaneously. Then, the learnt encoder and perturbation distribution are published.

Table 6: Inf²Guard results against DRAs. A smaller SSIM or PSNR indicates better defense performance ($\lambda = 0.4$).

CIFAR10			CIFAR100			Activity		
Scale ϵ	Utility	SSIM/PSNR	ϵ	Utility	SSIM/PSNR	ϵ	Utility	MSE
0	89.5%	0.78 / 15.97	0	52.7%	0.92 / 22.79	0	95.1%	0.81
0.75	85.2%	0.42 / 12.09	0.75	49.1%	0.36 / 13.36	0.5	90.1%	1.06
1.25	78.0%	0.21 / 11.87	1.00	46.5%	0.19 / 12.70	1.0	85.6%	1.32
1.75	68.9%	0.17 / 11.21	1.25	43.3%	0.14 / 12.29	1.5	81.0%	1.64

Table 7: Impact of λ on Inf²Guard against DRAs ($\epsilon = 1.25$).

CIFAR10			CIFAR100			Activity		
λ	Utility	SSIM/PSNR	λ	Utility	SSIM/PSNR	λ	Utility	MSE
0.1	83.2%	0.52 / 12.79	0.1	46.8%	0.46 / 14.75	0.1	90.0%	1.25
0.4	78.0%	0.21 / 11.87	0.4	46.5%	0.21 / 12.70	0.4	85.6%	1.32
0.7	67.9%	0.15 / 11.43	0.7	46.5%	0.20 / 12.42	0.7	85.0%	1.62

- **Attack training:** We mimic the strongest DRA, where the attacker knows the reconstruction protection network, training set, and perturbation distribution. S/he feeds each training data to the learnt encoder + perturbation distribution to get the perturbed representation. Then the attacker trains the reconstruction network (using the pair of input data and its perturbed representation) to infer the training data.

- **Defense/attack testing:** We use the utility test set to obtain the utility via querying the encoder and utility network; and use the attack test set to obtain the DRA performance by querying the trained encoder and reconstruction network.

Privacy metric: For image datasets, we use the common Structural Similarity Index Measure (SSIM) and PSNR metrics [30]. A larger SSIM (or PSNR) between two images indicate they look more similar. An effective attack aims to achieve a large SSIM (or PSNR), while the defender does the opposite. For human activity dataset, we use the mean-square error (MSE) between two samples to measure similarity. A smaller/larger MSE indicates a more effective attack/defense.

5.3.2 Experimental results

Utility-privacy results: Table 6 shows the defense results of Inf²Guard with the Gaussian perturbation distribution, where $\lambda = 0.4$ in Equation (20). We can observe ϵ acts a utility-privacy tradeoff. A larger ϵ implies adding more perturbation to the representation during defense training. This makes the DRA more challenging, but also sacrifice the utility more.

We also test the impact of λ and the results are shown in Table 7. We can see λ also acts as a tradeoff—a larger λ can protect data privacy more, while having larger utility loss.

Comparing with the DP-based defense: All empirical defenses against DRAs are broken are by an advanced attack [9]. A few papers [7, 56] show if a randomized algorithm satisfies DP, it can defend against DRAs with provable guarantees. We compare Inf²Guard with DP and Table 8 shows the DP results. Viewing with results in Table 6, we see Inf²Guard obtains better utility-privacy tradeoffs than DP-SGD.

Table 8: DP-SGD defense results against DRAs. A smaller SSIM or PSNR indicates better defense performance.

CIFAR10			CIFAR100			Activity	
Scale ϵ	Utility	SSIM/PSNR	ϵ	Utility	SSIM/PSNR	ϵ	Utility
0	89.5%	0.78 / 15.97	0	52.7%	0.92 / 22.79	0	95.1%
0.75	85.6%	0.50 / 13.21	0.75	49.5%	0.43 / 13.77	0.5	91.8%
1.25	77.4%	0.37 / 12.45	1.00	46.7%	0.24 / 12.87	1.0	90.1%
1.75	65.3%	0.36 / 12.35	1.25	43.3%	0.18 / 12.54	1.5	84.1%



(a) Raw images (b) No defense (c) DP (d) Inf^2Guard

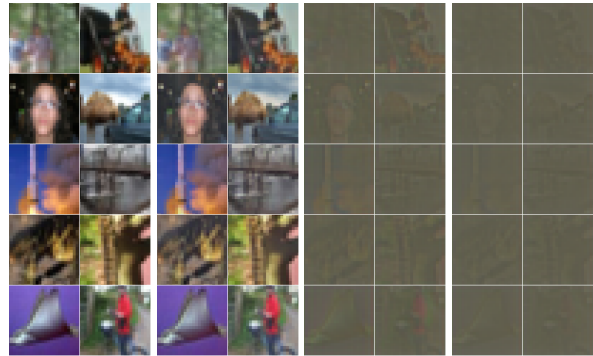
Figure 9: Raw images vs. reconstructions on CIFAR10. DP Utility: 77%, Inf^2Guard Utility: 78%.

Visualizing data reconstruction results: Figure 9 and Figure 10 show the reconstruction results on some CIFAR10 and CIFAR100 images, respectively. We see that, without defense, the attacker can accurately reconstruct the raw images. With a similar utility, visually, Inf^2Guard can better defend against image reconstruction than DP. Figure 11 summarizes the reconstruction results on 50 samples in Activity, where we report the difference between each reconstructed feature by Inf^2Guard and that by DP to the true feature. A (larger) positive value implies Inf^2Guard is (more) dissimilar than DP to the true feature. We can see Inf^2Guard has better defense results than DP in most (413 out of 516) of the features.

6 Discussion and Future Work

Inf^2Guard and DP: Essentially, Inf^2Guard and DP are two different provable privacy mechanisms, and they complement each other. First, DP mainly measures the user or sample-level privacy risks in the worst case while Inf^2Guard can accurately measure the average privacy risks at the dataset level with the derived bounds. Second, DP has been shown to provide some resilience transferability across some inference attacks [56] (but not all of them). It is also interesting to study the resilience transferability for the proposed Inf^2Guard , which we will explore in the future. More importantly, our Inf^2Guard can complement DP. For instance, we can use the learnt (deterministic) data representations by Inf^2Guard as input to DP-SGD or add (Gaussian) noise to the representations to ensure DP guarantees against MIAs.

Task-agnostic representation learning: Our current MI formulation for utility preservation knows the labels of the learn-



(a) Raw images (b) No defense (c) DP (d) Inf^2Guard

Figure 10: Raw images vs. reconstructions on CIFAR100. DP Utility: 47%, Inf^2Guard Utility: 47%. Better zoom in.

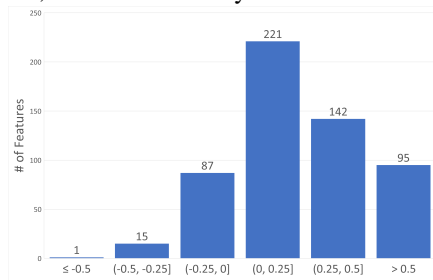


Figure 11: Inf^2Guard vs. DP on 50 samples in Activity (both utility=86%). We count #features located in each bin. The value range in each bin means the difference between the reconstructed feature by Inf^2Guard and that by DP to the true feature. A positive value implies Inf^2Guard produces more dissimilar reconstruction than DP.

ing task (e.g., see Equation (2)). A more promising solution would be task-agnostic, i.e., learning task-agnostic representations that can benefit many (unknown) downstream tasks. We note that our framework can be easily extended to this scenario. For instance, in MIAs, we now require the learnt representation \mathbf{r} includes as much information about the *training* sample \mathbf{x} as possible (i.e., $u = 1$). Intuitively, when \mathbf{r} retains all information about \mathbf{x} , the model trained on \mathbf{r} will have the same performance as trained on the raw \mathbf{x} , despite the learning task. Formally, the MI objective becomes $\max_{\mathcal{I}} I(\mathbf{x}; \mathbf{r} | u = 1)$.

Defending against multiple inference attacks simultaneously: We design the customized MI objectives to defend against each inference attack in the paper. A natural solution to defend against multiple inference attacks is unifying their training objectives (by summarizing them with tradeoff hyperparameters). While this is possible, we emphasize that the learnt encoder is weak against all attacks. This is because the encoder should balance the defense effectiveness among these attacks, and cannot be optimal against all of them.

Generalizing our theoretical results: Our theoretical results assume the learning task is binary classification and dataset property is binary-valued. We will generalize our theoretical results to multiclass classification and other types of learning such as regression, and multi-valued dataset property.

Generalizing our framework against security attacks: In our current framework, each privacy protection task is formalized via an MI objective. An important future work would be generalizing our framework to design customized MI objectives to learn robust representations against security attacks such as evasion, poisoning, and backdoor attacks.

7 Related Work

7.1 MIAs and Defenses

MIAs [13, 15, 17, 34, 42, 57, 61–63, 73, 76, 79]. Existing MIAs can be classified as *training based* [13, 15, 17, 42, 55, 57, 61, 63, 75, 76] and *non-training based* [17, 62]. Given a (non)training sample and its output by a target ML model, training based MIAs use the (sample, output) pair to train a binary classifier, which is then used to determine whether a testing sample belongs to the training set or not. For instance, [61] introduces multiple shadow models to perform training. In contrast, non-training based MIAs directly use the samples’ predicted score/label to make decisions. For instance, [62] designs a metric *prediction correctness*, which infers the membership based on whether a given sample is correctly classified by the target model or not. Overall, an MIA that has more information is often more effective than that has less information.

Defenses [38, 48, 57, 59, 61, 62, 64, 74]. They can be categorized as *training time* based defense (e.g., dropout [57], L_2 norm regularization [61], model stacking [57], adversary regularization [48], loss variance deduction [74], DP [3, 35, 78], early stopping [62], knowledge distillation [59]) and *inference time* based defense (e.g., MemGuard [38]). Almost all of them are empirical and broken by stronger attacks [17, 62]. DP is only defense offering privacy guarantees. Its main idea is to add noise to the gradient [3, 78] or objective function [35] during training. The main drawback of current DP methods is that they have significant utility losses [36, 59].

7.2 PIAs and Defenses

PIAs [5, 6, 14, 22, 27, 44, 45, 66, 69, 80, 82]. Ateniese et al. [6] are the first to describe the problem of the PIA (against support vector machines and hidden Markov models), where the attack is performed in the the white-box setting and consists of training a meta-classifier on top of many shadow models. Ganju et al. [22] extend PIAs to neural networks, particularly fully connected neural networks (FCNNs). Zhang et al. [80] propose PIAs in the black-box setting and train a meta-classifier based on shadow models. Mahlouiifar et al. [44] observe that data poisoning attacks can be incorporated into training the shadow model and increase the effectiveness of PIAs. Suri and Evans [66] are the first to formally formalize PIAs as a cryptographic game, inspired by the way to formalize MIAs [76]. They also extend the white-box attack on FCNNs [22] to convolutional neural networks (CNNs). Zhou et al. [82] develop

the first PIA against generative models, i.e., generative adversarial networks (GANs) [26], under the black-box setting. Chaudhari et al. [14] propose a data poisoning strategy to perform the efficient private property inference.

Defenses. To our best knowledge, there exist no known effective defenses against PIAs. DP cannot mitigate PIAs since it obfuscates individual samples, while PIAs care about the entire datasets [66]. [66] also shows that DP does not work as a potential defense (also verified in Section 5).

7.3 DRAs and Defenses

DRAs [7–9, 21, 24, 30, 31, 37, 70, 71, 77, 81, 84]. Existing DRAs mainly reconstruct the training data from the model parameters or representations. They are formulated as an optimization problem that minimizes the difference between gradient from the raw training data and that from the reconstructed data. For instance, Zhu et al. [84] proposed a DLG attack method which relies entirely on minimization of the difference of gradients. Furthermore, several methods [24, 31, 37, 70, 77] propose to incorporate prior knowledge (e.g., total variation regularization [24, 77], batch normalization statistics [77]) into the training data, or introduce an auxiliary dataset to simulate the training data distribution [31, 37, 70] (e.g., via GANs [26]). A few works [24, 83] derive close-formed solutions to reconstruct the data, by constraining the neural networks to be fully connected [24] or convolutional [83].

Defenses [23, 28, 41, 51, 58, 65, 72, 84]. Most of these defenses have none/little privacy guarantees. For instance, Zhu et al. [84] propose to prune model parameters with smaller magnitudes. Sun et al. [65] propose to obfuscate the gradient for a single layer (called defender layer) such that the reconstructed data and the original data are dissimilar. Gao et al. [23] propose to generate augmented images that, when they are used to train the network, produce non-invertible gradients. These defenses are broken by an advanced attack based on Bayesian learning [9]. Only defenses based on DP-SGD [3], a version of SGD with clipping and adding Gaussian noise, provide formal privacy guarantees.

8 Conclusion

We propose a unified information-theoretic framework, dubbed Inf^2Guard , to learn privacy-preserving representations against the three major types of inferences attacks (i.e., membership inference, property inference, and data reconstruction attacks). The framework formalizes the utility preservation and privacy protection against each attack via customized mutual information objectives. The framework also enables deriving theoretical results, e.g., inherent utility-privacy tradeoff, and guaranteed privacy leakage against each attack. Extensive evaluations verify the effectiveness of Inf^2Guard for learning privacy-preserving representations and show the superiority over the compared baselines.

Acknowledgement

We thank all the anonymous reviewers and our shepherd for the valuable feedback and constructive comments. Wang is partially supported by the National Science Foundation (NSF) under grant Nos. ECCS-2216926, CNS-2241713, and CNS-2339686. Hong is partially supported by the National Science Foundation (NSF) under grant Nos. CNS-2302689, CNS-2308730, CNS-2319277 and CMMI-2326341. Any opinions, findings and conclusions or recommendations expressed in this material are those of the author(s) and do not necessarily reflect the views of the funding agencies.

References

- [1] Chatgpt. <https://chat.openai.com/>. developed by OpenAI.
- [2] Palm 2. <https://ai.google/discover/palm2/>. developed by Google.
- [3] Martin Abadi, Andy Chu, Ian Goodfellow, H Brendan McMahan, Ilya Mironov, Kunal Talwar, and Li Zhang. Deep learning with differential privacy. In *CCS*, 2016.
- [4] Alexander A Alemi, Ian Fischer, Joshua V Dillon, and Kevin Murphy. Deep variational information bottleneck. In *ICLR*, 2017.
- [5] Caridad Arroyo Arevalo, Sayedeh Leila Noorbakhsh, Yun Dong, Yuan Hong, and Binghui Wang. Task-agnostic privacy-preserving representation learning for federated learning against attribute inference attacks. In *AAAI*, 2024.
- [6] Giuseppe Ateniese, Luigi V Mancini, Angelo Spognardi, Antonio Villani, Domenico Vitali, and Giovanni Felici. Hacking smart machines with smarter ones: How to extract meaningful data from machine learning classifiers. *IJSN*, 2015.
- [7] Borja Balle, Giovanni Cherubin, and Jamie Hayes. Reconstructing training data with informed adversaries. In *IEEE SP*, 2022.
- [8] Mislav Balunovic, Dimitar Dimitrov, Nikola Jovanović, and Martin Vechev. Lamp: Extracting text from gradients with language model priors. In *NeurIPS*, 2022.
- [9] Mislav Balunovic, Dimitar Iliev Dimitrov, Robin Staab, and Martin Vechev. Bayesian framework for gradient leakage. In *ICLR*, 2022.
- [10] Mohamed Ishmael Belghazi, Aristide Baratin, Sai Rajeshwar, Sherjil Ozair, Yoshua Bengio, Aaron Courville, and Devon Hjelm. Mutual information neural estimation. In *ICML*, 2018.
- [11] Yoshua Bengio, Aaron Courville, and Pascal Vincent. Representation learning: A review and new perspectives. *IEEE TPMAI*, 2013.
- [12] Chris Calabro. *The exponential complexity of satisfiability problems*. University of California, San Diego, 2009.
- [13] Nicholas Carlini, Steve Chien, Milad Nasr, Shuang Song, Andreas Terzis, and Florian Tramèr. Membership inference attacks from first principles. In *IEEE SP*, 2022.
- [14] Harsh Chaudhari, John Abascal, Alina Oprea, Matthew Jagielski, Florian Tramèr, and Jonathan Ullman. Snap: Efficient extraction of private properties with poisoning. In *IEEE SP*, 2023.
- [15] Dingfan Chen, Ning Yu, Yang Zhang, and Mario Fritz. Ganleaks: A taxonomy of membership inference attacks against generative models. In *CCS*, 2020.
- [16] Pengyu Cheng, Weituo Hao, Shuyang Dai, Jiachang Liu, Zhe Gan, and Lawrence Carin. Club: A contrastive log-ratio upper bound of mutual information. In *ICML*, 2020.
- [17] Christopher A Choquette-Choo, Florian Tramèr, Nicholas Carlini, and Nicolas Papernot. Label-only membership inference attacks. In *ICML*, 2021.
- [18] Clarifai. <https://www.clarifai.com/demo>. July 2019.
- [19] John C Duchi and Martin J Wainwright. Distance-based and continuum fano inequalities with applications to statistical estimation. *arXiv preprint arXiv:1311.2669*, 2013.
- [20] Cynthia Dwork. Differential privacy. In *ICALP*, 2006.
- [21] Liam H Fowl, Jonas Geiping, Wojciech Czaja, Micah Goldblum, and Tom Goldstein. Robbing the fed: Directly obtaining private data in federated learning with modified models. In *ICLR*, 2022.
- [22] Karan Ganju, Qi Wang, Wei Yang, Carl A Gunter, and Nikita Borisov. Property inference attacks on fully connected neural networks using permutation invariant representations. In *CCS*, 2018.
- [23] Wei Gao, Shangwei Guo, Tianwei Zhang, Han Qiu, Yonggang Wen, and Yang Liu. Privacy-preserving collaborative learning with automatic transformation search. In *CVPR*, 2021.
- [24] Jonas Geiping, Hartmut Bauermeister, Hannah Dröge, and Michael Moeller. Inverting gradients—how easy is it to break privacy in federated learning? In *NeurIPS*, 2020.
- [25] Alison L Gibbs and Francis Edward Su. On choosing and bounding probability metrics. *International statistical review*, 70(3):419–435, 2002.
- [26] Ian Goodfellow, Jean Pouget-Abadie, Mehdi Mirza, Bing Xu, David Warde-Farley, Sherjil Ozair, Aaron Courville, and Yoshua Bengio. Generative adversarial nets. In *NIPS*, 2014.
- [27] Divya Gopinath, Hayes Converse, Corina Pasareanu, and Ankur Taly. Property inference for deep neural networks. In *ASE*, 2019.
- [28] Jihun Hamm, Yingjun Cao, and Mikhail Belkin. Learning privately from multiparty data. In *ICML*, 2016.
- [29] Valentin Hartmann, Léo Meynert, Maxime Peyrard, Dimitrios Dimitriadis, Shruti Tople, and Robert West. Distribution inference risks: Identifying and mitigating sources of leakage. In *IEEE SaTML*, 2023.
- [30] Zecheng He, Tianwei Zhang, and Ruby B Lee. Model inversion attacks against collaborative inference. In *ACSAC*, 2019.
- [31] Briland Hitaj, Giuseppe Ateniese, and Fernando Perez-Cruz. Deep models under the gan: information leakage from collaborative deep learning. In *CCS*, 2017.

- [32] R Devon Hjelm, Alex Fedorov, Samuel Lavoie-Marchildon, Karan Grewal, Phil Bachman, Adam Trischler, and Yoshua Bengio. Learning deep representations by mutual information estimation and maximization. In *ICLR*, 2019.
- [33] Nils Homer, Szabolcs Szelinger, Margot Redman, David Duggan, Waibhav Tembe, Jill Muehling, John V Pearson, Dietrich A Stephan, Stanley F Nelson, and David W Craig. Resolving individuals contributing trace amounts of dna to highly complex mixtures using high-density snp genotyping microarrays. *PLoS genetics*.
- [34] Bo Hui, Yuchen Yang, Haolin Yuan, Philippe Burlina, Neil Zhenqiang Gong, and Yinzhi Cao. Practical blind membership inference attack via differential comparisons. In *NDSS*, 2021.
- [35] Roger Iyengar, Joseph P Near, Dawn Song, Om Thakkar, Abhradeep Thakurta, and Lun Wang. Towards practical differentially private convex optimization. In *IEEE SP*, 2019.
- [36] Bargav Jayaraman and David Evans. Evaluating differentially private machine learning in practice. In *USENIX Security*, 2019.
- [37] Jinwoo Jeon, Jaechang Kim, Kangwook Lee, Sewoong Oh, and Jungseul Ok. Gradient inversion with generative image prior. In *NeurIPS*, 2021.
- [38] Jinyuan Jia, Ahmed Salem, Michael Backes, Yang Zhang, and Neil Zhenqiang Gong. Memguard: Defending against black-box membership inference attacks via adversarial examples. In *CCS*, 2019.
- [39] Diederik P Kingma and Max Welling. Auto-encoding variational {Bayes}. In *ICLR*, 2014.
- [40] Alex Krizhevsky. Learning multiple layers of features from tiny images. Technical report, 2009.
- [41] Hongkyu Lee, Jeehyeong Kim, Seyoung Ahn, Rasheed Husain, Sunghyun Cho, and Junggab Son. Digestive neural networks: A novel defense strategy against inference attacks in federated learning. *Computers & Security*, 2021.
- [42] Klas Leino and Matt Fredrikson. Stolen memories: Leveraging model memorization for calibrated white-box membership inference. In *Usenix Security*, 2020.
- [43] Ziwei Liu, Ping Luo, Xiaogang Wang, and Xiaoou Tang. Deep learning face attributes in the wild. In *ICCV*, 2015.
- [44] Saeed Mahloujifar, Esha Ghosh, and Melissa Chase. Property inference from poisoning. In *IEEE SP*, 2022.
- [45] Pratyush Maini, Mohammad Yaghini, and Nicolas Papernot. Dataset inference: Ownership resolution in machine learning. In *ICLR*, 2021.
- [46] Ilya Mironov. Rényi differential privacy. In *IEEE CSF*, 2017.
- [47] Meisam Mohammady, Shangyu Xie, Yuan Hong, Mengyuan Zhang, Lingyu Wang, Makan Pourzandi, and Mourad Debbabi. R2DP: A universal and automated approach to optimizing the randomization mechanisms of differential privacy for utility metrics with no known optimal distributions. In *CCS*, 2020.
- [48] Milad Nasr, Reza Shokri, and Amir Houmansadr. Machine learning with membership privacy using adversarial regularization. In *CCS*, 2018.
- [49] Sebastian Nowozin, Botond Cseke, and Ryota Tomioka. f-gan: Training generative neural samplers using variational divergence minimization. In *NIPS*, 2016.
- [50] Aaron van den Oord, Yazhe Li, and Oriol Vinyals. Representation learning with contrastive predictive coding. *arXiv*, 2018.
- [51] Manas Pathak, Shantanu Rane, and Bhiksha Raj. Multiparty differential privacy via aggregation of locally trained classifiers. In *NeurIPS*, 2010.
- [52] Xue Bin Peng, Angjoo Kanazawa, Sam Toyer, Pieter Abbeel, and Sergey Levine. Variational discriminator bottleneck: Improving imitation learning, inverse rl, and gans by constraining information flow. *arXiv preprint arXiv:1810.00821*, 2018.
- [53] Ben Poole, Sherjil Ozair, Aaron van den Oord, Alexander A Alemi, and George Tucker. On variational bounds of mutual information. In *ICML*, 2019.
- [54] Jorge Reyes-Ortiz, Davide Anguita, Alessandro Ghio, Luca Oneto, and Xavier Parra. Human Activity Recognition Using Smartphones. UCI Machine Learning Repository, 2012. DOI: <https://doi.org/10.24432/C54S4K>.
- [55] Alexandre Sablayrolles, Matthijs Douze, Cordelia Schmid, Yann Ollivier, and Hervé Jégou. White-box vs black-box: Bayes optimal strategies for membership inference. In *ICML*, 2019.
- [56] Ahmed Salem, Giovanni Cherubin, David Evans, Boris Köpf, Andrew Paverd, Anshuman Suri, Shruti Tople, and Santiago Zanella-Béguelin. Sok: Let the privacy games begin! a unified treatment of data inference privacy in machine learning. In *IEEE SP*, 2023.
- [57] Ahmed Salem, Yang Zhang, Mathias Humbert, Pascal Berrang, Mario Fritz, and Michael Backes. MI-leaks: Model and data independent membership inference attacks and defenses on machine learning models. In *NDSS*, 2018.
- [58] Daniel Scheliga, Patrick Mäder, and Marco Seeland. Precode-a generic model extension to prevent deep gradient leakage. In *WACV*, 2022.
- [59] Virat Shejwalkar and Amir Houmansadr. Membership privacy for machine learning models through knowledge transfer. In *AAAI*, 2021.
- [60] Reza Shokri and Vitaly Shmatikov. Privacy-preserving deep learning. In *CCS*, 2015.
- [61] Reza Shokri, Marco Stronati, Congzheng Song, and Vitaly Shmatikov. Membership inference attacks against machine learning models. In *IEEE SP*, 2017.
- [62] Liwei Song and Prateek Mittal. Systematic evaluation of privacy risks of machine learning models. In *USENIX Security*, 2021.
- [63] Liwei Song, Reza Shokri, and Prateek Mittal. Privacy risks of securing machine learning models against adversarial examples. In *CCS*, 2019.
- [64] Nitish Srivastava, Geoffrey E Hinton, Alex Krizhevsky, Ilya Sutskever, and Ruslan Salakhutdinov. Dropout: a simple way to prevent neural networks from overfitting. *JMLR*, 2014.

- [65] Jingwei Sun, Ang Li, Binghui Wang, Huanrui Yang, Hai Li, and Yiran Chen. Provable defense against privacy leakage in federated learning from representation perspective. In *CVPR*, 2021.
- [66] Anshuman Suri and David Evans. Formalizing and estimating distribution inference risks. In *PETS*, 2022.
- [67] Laurens Van der Maaten and Geoffrey Hinton. Visualizing data using t-sne. *JMLR*, 2008.
- [68] Han Wang, Jayashree Sharma, Shuya Feng, Kai Shu, and Yuan Hong. A model-agnostic approach to differentially private topic mining. In *KDD*, 2022.
- [69] Xiuling Wang and Wendy Hui Wang. Group property inference attacks against graph neural networks. In *CCS*, 2022.
- [70] Zhibo Wang, Mengkai Song, Zhifei Zhang, Yang Song, Qian Wang, and Hairong Qi. Beyond inferring class representatives: User-level privacy leakage from federated learning. In *INFOCOM*, 2019.
- [71] Zihan Wang, Jason Lee, and Qi Lei. Reconstructing training data from model gradient, provably. In *AISTATS*, 2023.
- [72] Kang Wei, Jun Li, Ming Ding, Chuan Ma, Howard H Yang, Farhad Farokhi, Shi Jin, Tony QS Quek, and H Vincent Poor. Federated learning with differential privacy: Algorithms and performance analysis. *IEEE TIFS*, 2020.
- [73] Yuxin Wen, Arpit Bansal, Hamid Kazemi, Eitan Borgnia, Micah Goldblum, Jonas Geiping, and Tom Goldstein. Canary in a coalmine: Better membership inference with ensembled adversarial queries. In *ICLR*, 2023.
- [74] Nuo Xu, Binghui Wang, Ran Ran, Wujie Wen, and Parv Venkatasubramaniam. Neuguard: Lightweight neuron-guided defense against membership inference attacks. In *ACSAC*, 2022.
- [75] Jiayuan Ye, Aadyaa Maddi, Sasi Kumar Murakonda, Vincent Bindschaedler, and Reza Shokri. Enhanced membership inference attacks against machine learning models. In *CCS*, 2022.
- [76] Samuel Yeom, Irene Giacomelli, Matt Fredrikson, and Somesh Jha. Privacy risk in machine learning: Analyzing the connection to overfitting. In *IEEE CSF*, 2018.
- [77] Hongxu Yin, Arun Mallya, Arash Vahdat, Jose M Alvarez, Jan Kautz, and Pavlo Molchanov. See through gradients: Image batch recovery via gradinversion. In *CVPR*, 2021.
- [78] Lei Yu, Ling Liu, Calton Pu, Mehmet Emre Gursoy, and Stacey Truex. Differentially private model publishing for deep learning. In *IEEE SP*, 2019.
- [79] Xiaoyong Yuan and Lan Zhang. Membership inference attacks and defenses in neural network pruning. In *Usenix Security*, 2022.
- [80] Wanrong Zhang, Shruti Tople, and Olga Ohrimenko. Leakage of dataset properties in multi-party machine learning. In *USENIX Security*, 2021.
- [81] Bo Zhao, Konda Reddy Mopuri, and Hakan Bilen. idlg: Improved deep leakage from gradients. *arXiv*, 2020.
- [82] Junhao Zhou, Yufei Chen, Chao Shen, and Yang Zhang. Property inference attacks against gans. *NDSS 2022*, 2022.

Algorithm 1 Inf^2Guard against MIAs

Input: Dataset D_1 of members and dataset D_0 of non-members, tradeoff hyperparameter $\lambda \in [0, 1]$, learning rates lr_1, lr_2, lr_3 ; #local gradients I , #global rounds T .

Output: Network parameters: Θ, Ψ, Ω .

- 1: Initialize Θ, Ψ, Ω for the encoder f , membership protection network g_Ψ , and utility preservation network h_Φ ;
 - 2: **for** $t = 1$ to T **do**
 - 3: $L_1 = \sum_{(\mathbf{x}_j, u_j) \in D_1 \cup D_0} H(u_j, g_\Psi(f(\mathbf{x}_j)))$;
 - 4: $L_2 = \sum_{(\mathbf{x}_j, y_j) \in D_1} H(y_j, h_\Omega(f(\mathbf{x}_j)))$;
 - 5: **for** $i = 1$ to I **do**
 - 6: $\Psi \leftarrow \Psi - lr_1 \cdot \frac{\partial L_1}{\partial \Psi}$;
 - 7: $\Omega \leftarrow \Omega - lr_2 \cdot \frac{\partial L_2}{\partial \Omega}$;
 - 8: $\Theta \leftarrow \Theta + lr_3 \cdot \frac{\partial (\lambda L_1 - (1-\lambda)L_2)}{\partial \Theta}$;
-

Algorithm 2 Inf^2Guard against PIAs

Input: N datasets $\{D_j\}_{j=1}^N$ sampled from a reference dataset D_r with each D_j having a property value u_j , tradeoff hyperparameter $\lambda \in [0, 1]$, learning rates lr_1, lr_2, lr_3 ; #local gradients I , #global rounds T .

Output: Network parameters: Θ, Ω, Ψ .

- 1: Initialize Θ, Ψ, Ω for the encoder f , property protection network g_Ψ , and utility preservation network h_Φ ;
 - 2: **for** round $t = 1$ to T **do**
 - 3: $L_1 = \sum_{\{(\mathbf{x}_j, y_j) = D_j\}_j} H(u_j, g_\Psi(f(\mathbf{X}_j)))$;
 - 4: $L_2 = \sum_{(\mathbf{x}_i, y_i) \in \cup_j D_j} H(y_i, h_\Omega(f(\mathbf{x}_i)))$;
 - 5: **for** $i = 1$ to I **do**
 - 6: $\Psi \leftarrow \Psi - lr_1 \cdot \frac{\partial L_1}{\partial \Psi}$;
 - 7: $\Omega \leftarrow \Omega - lr_2 \cdot \frac{\partial L_2}{\partial \Omega}$;
 - 8: $\Theta \leftarrow \Theta + lr_3 \cdot \frac{\partial (\lambda L_1 - (1-\lambda)L_2)}{\partial \Theta}$;
-

Algorithm 3 Update perturbation distribution parameter Φ

Input: K Monte Carlo samples, the encoder f_Θ in the previous round, objective function Eqn (20), learning rate lr , #epochs I_l

Output: Perturbation distribution parameters Φ

- 1: Initialize $\Phi = (\boldsymbol{\mu}, \boldsymbol{\sigma})$.
 - 2: **for** $i = 1$ to I_l **do**
 - 3: **for** $j = 1$ to K **do**
 - 4: Sample \mathbf{z}_j from $\mathcal{N}(0, 1)$ and compute $\boldsymbol{\delta}_j = \boldsymbol{\mu} + \boldsymbol{\sigma}\mathbf{z}_j$;
 - 5: Calculate the gradient \mathbf{g}_Φ of Eqn (25) w.r.t. Φ ;
 - 6: Update Φ by: $\Phi \leftarrow \Phi - lr \cdot \mathbf{g}_\Phi$.
-

[83] Junyi Zhu and Matthew Blaschko. R-gap: Recursive gradient attack on privacy. *ICLR*, 2021.

[84] Ligeng Zhu, Zhijian Liu, and Song Han. Deep leakage from gradients. In *NeurIPS*, 2019.

A Proofs of Privacy Guarantees

The following lemmas will be useful in the proofs.

Lemma 1 ([12] Theorem 2.2). *Let $H_2^{-1}(p)$ be the inverse binary entropy function for $p \in [0, 1]$, then $H_2^{-1}(p) \geq \frac{p}{2 \log_2(6/p)}$.*

Lemma 2 (Data processing inequality). *Given random variables X, Y , and Z that form a Markov chain in the order $X \rightarrow Y \rightarrow Z$, then the mutual information between X and Y is greater than or equal to the mutual information between X and Z . That is $I(X; Y) \geq I(X; Z)$.*

Algorithm 4 Inf^2Guard against DRAs

Input: A dataset $D = \{\mathbf{x}_n, y_n\}$, hyperparameters $\lambda \in [0, 1]$, learning rates lr_1, lr_2, lr_3 , #local gradients l , #global rounds T .

Output: Network parameters: Ω, Ψ, Θ .

- 1: Initialize $\Theta, \Psi, \Omega, \Phi$ for the encoder f , data reconstruction network g_Ψ , utility preservation network h_Ω , and perturbation distribution parameter.
 - 2: **for** round $t = 1$ to T **do**
 - 3: **for** each batch $bs \subset D$ **do**
 - 4: **Update** Φ via Algorithm 3;
 - 5: **Update** g_Ψ (given Θ and $\{\delta_i\}$): Calculate $I_{\Theta, \Psi}^{(JSD)}$ on bs with $\{\delta_i\}$ via Eqn (22); $\Psi \leftarrow \Psi + lr_1 \cdot \partial I_{\Theta, \Psi}^{(JSD)} / \partial \Psi$;
 - 6: **Update** h_Ω (given Θ and $\{\delta_i\}$): Calculate CE loss L_1 on bs with $\{\delta_i\}$ via Eqn (23); Calculate CE loss L_2 on bs with clean data via Eqn (24); $\Omega \leftarrow \Omega - lr_2 \cdot \partial(L_1 + L_2) / \partial \Omega$;
 - 7: **Update** f_Θ (given Ψ, Ω , and $\{\delta_i\}$): $\Theta \leftarrow \Theta - lr_3 \cdot \frac{\partial}{\partial \Theta} (\lambda I_{\Theta, \Psi}^{(JSD)} + (1 - \lambda)(L_1 + L_2))$;
-

A.1 Proof of Theorem 1 for MIAs

Theorem 1. Let f be the learnt encoder by Equation (6) over a data distribution $\mathcal{D} \subset \mathcal{X}$. For a random data sample $\mathbf{x} \sim \mathcal{D}$ with the learnt representation $\mathbf{r} = f(\mathbf{x})$ and membership u , we have $\Pr(A_{MIA}(\mathbf{r}) = u) \leq 1 - \frac{H(u|\mathbf{r})}{2\log_2(6/H(u|\mathbf{r}))}$, $\forall A_{MIA} \in \mathcal{A}_{MIA}$.

Proof. For brevity, we define the optimal MIA as A^* . Let s be an indicator that takes value 1 if and only if $A^*(\mathbf{r}) \neq u$, and 0 otherwise, i.e., $s = 1[A^*(\mathbf{r}) \neq u]$. Now consider the conditional entropy $H(s, u|A^*(\mathbf{r}))$. By decomposing it via two different ways, we have

$$\begin{aligned} H(s, u|A^*(\mathbf{r})) &= H(u|A^*(\mathbf{r})) + H(s|u, A^*(\mathbf{r})) \\ &= H(s|A^*(\mathbf{r})) + H(u|s, A^*(\mathbf{r})), \end{aligned} \quad (26)$$

Note that $H(s|u, A^*(\mathbf{r})) = 0$ as when u and $A^*(\mathbf{r})$ are known, s is also known. Moreover,

$$\begin{aligned} H(u|s, A^*(\mathbf{r})) &= \Pr(s=1)H(u|s=1, A^*(\mathbf{r})) + \Pr(s=0)H(u|s=0, A^*(\mathbf{r})) \\ &= 0 + 0 = 0, \end{aligned} \quad (27)$$

because when knowing s and $A^*(\mathbf{r})$, we also know u .

Thus, Equation 26 reduces to $H(u|A^*(\mathbf{r})) = H(s|A^*(\mathbf{r}))$. As conditioning does not increase entropy, i.e., $H(s|A^*(\mathbf{r})) \leq H(s)$, we further have

$$H(u|A^*(\mathbf{r})) \leq H(s). \quad (28)$$

On the other hand, using mutual information and entropy properties, we have $I(u; A^*(\mathbf{r})) = H(u) - H(u|A^*(\mathbf{r}))$ and $I(u; \mathbf{r}) = H(u) - H(u|\mathbf{r})$. Hence,

$$I(u; A^*(\mathbf{r})) + H(u|A^*(\mathbf{r})) = I(u; \mathbf{r}) + H(u|\mathbf{r}). \quad (29)$$

Note that $u \perp A^*(\mathbf{r})|\mathbf{r}$. Hence, we have the Markov chain $u \rightarrow \mathbf{r} \rightarrow A^*(\mathbf{r})$. Based on the data processing inequality in Lemma 2, $I(u; A^*(\mathbf{r})) \leq I(u; \mathbf{r})$. Combining it with Equation 29, we have

$$H(u|A^*(\mathbf{r})) \geq H(u|\mathbf{r}). \quad (30)$$

Combing Equations 28 and 30, we have $H(s) = H_2(\Pr(s =$

$1)) \geq H(u|\mathbf{r})$, which implies

$$\Pr(A^*(\mathbf{r}) \neq u) = \Pr(s = 1) \geq H_2^{-1}(H(u|\mathbf{r})), \quad (31)$$

where $H_2(t) = -t \log_2 t - (1-t) \log_2 (1-t)$.

Finally, by applying Lemma 1, we have

$$\Pr(A^*(\mathbf{r}) \neq u) \geq \frac{H(u|\mathbf{r})}{2\log_2(6/H(u|\mathbf{r}))}. \quad (32)$$

Hence the membership privacy leakage is bounded by $\Pr(A^*(\mathbf{r}) = u) \leq 1 - \frac{H(u|\mathbf{r})}{2\log_2(6/H(u|\mathbf{r}))}$. \square

A.2 Proof of Theorem 2 for PIAs

Theorem 2. Let f be the learnt encoder by Equation (11) over a data distribution \mathcal{D} . For a random dataset $\mathbf{X} \sim \mathcal{D}$ with the learnt representation $\mathbf{R} = f(\mathbf{X})$ and dataset property u , we have $\Pr(A_{PIA}(\mathbf{R}) = u) \leq 1 - \frac{H(u|\mathbf{R})}{2\log_2(6/H(u|\mathbf{R}))}$, $\forall A_{PIA} \in \mathcal{A}_{PIA}$.

Proof. The proof is identical to that for Theorem 1. The only differences are: 1) replace \mathbf{r} to be \mathbf{R} ; and 2) s is an indicator that takes value 1 if and only if $A(\mathbf{R}) \neq u$, and 0 otherwise, i.e., $s = 1[A(\mathbf{R}) \neq u]$, where u is the private dataset property. \square

A.3 Proof of Theorem 3 for DRAs

Different from MIAs and PIAs where the adversary makes decisions in a discrete space, i.e., inferring member or non-member and property value, DRAs aim to infer the *continuous* data. To deal with this challenging scenario, we need to first introduce the following lemma.

Recall that for a set \mathcal{S} in a d -dimension space, we denote $\partial\mathcal{S}$ as its boundary in the $(d-1)$ -dimensional space, and denote the volume of $\partial\mathcal{S}$ as $\text{Vol}(\partial\mathcal{S})$. For a $\mathbf{v} \in \mathcal{V}$, an l_p -norm ball centered at \mathbf{v} with a radius t as $\mathcal{B}_p(\mathbf{v}, t) = \{\mathbf{v}' \in \mathbb{R}^d : \|\mathbf{v}' - \mathbf{v}\|_p \leq t\}$.

Lemma 3 (Proposition 2 in [19]). Assume the set $\mathcal{V} \subset \mathbb{R}^d$ has a non-zero and finite volume. Then, if \mathbf{v} is uniform over \mathcal{V} and for any Markov chain $\mathbf{v} \rightarrow \dots \rightarrow \mathbf{w} \rightarrow \dots \rightarrow \mathbf{v}'$, we have $\Pr(\|\mathbf{v}' - \mathbf{v}\|_p \geq t) \geq 1 - \frac{I(\mathbf{v}; \mathbf{w}) + \log 2}{\log \text{Vol}(\partial\mathcal{V}) - \log \text{Vol}(\partial\mathcal{V}(t))}$, where $\text{Vol}(\partial\mathcal{V}(t)) = \max_{\mathbf{v} \in \mathcal{V}} \text{Vol}(\partial\mathcal{B}_p(\mathbf{v}, t) \cap \mathcal{V})$.

Now we prove the Theorem 3 restated as below.

Theorem 3. Let f be the encoder learnt by Equation (20) over a data distribution $\mathcal{D} \subset \mathcal{X}$ and δ be the perturbation for a random sample $\mathbf{x} \sim \mathcal{X}$. Then, $\Pr(\|A_{DRA}(\mathbf{r} + \delta) - \mathbf{x}\|_p \geq \eta) \geq 1 - \frac{I(\mathbf{x}; \mathbf{r} + \delta) + \log 2}{\log \text{Vol}(\partial\mathcal{X}) - \log \text{Vol}(\partial\mathcal{X}(\eta))}$, $\forall A_{DRA} \in \mathcal{A}_{DRA}$, where $\text{Vol}(\partial\mathcal{X}(\eta)) = \max_{\mathbf{x} \in \mathcal{X}} \text{Vol}(\partial\mathcal{B}_p(\mathbf{x}, \eta) \cap \mathcal{X})$.

Proof. We have the following Markov chain: $\mathbf{x} \rightarrow \mathbf{r} = f(\mathbf{x}) \rightarrow \mathbf{r} + \delta \rightarrow A_{DRA}(\mathbf{r} + \delta)$. W.l.o.g., we assume \mathbf{x} is uniform over the input set \mathcal{X} . We let $\mathbf{x} = \mathbf{v}$, $\mathbf{r} + \delta = \mathbf{w}$, and $A_{DRA}(\mathbf{r} + \delta) = \mathbf{v}'$. Then by applying Lemma 3, we reach out Theorem 3. \square

B Theoretical Utility-Privacy Tradeoff

B.1 Tradeoff of Inf^2 Guard against MIAs

Let \mathcal{A}_{MIA} be the set of all MIAs, i.e., $\mathcal{A}_{MIA} = \{A_{MIA} : \mathbf{r} = f(\mathbf{x}) \in \mathcal{Z} \rightarrow u \in \{0, 1\}\}$, with data \mathbf{x} randomly sampled from the data distribution \mathcal{D} . W.l.o.g, we assume the representation space \mathcal{Z} is bounded by R , i.e., $\max_{\mathbf{r} \in \mathcal{Z}} \|\mathbf{r}\| \leq R$. Remember the learning task classifier $C : \mathcal{Z} \rightarrow \mathcal{Y} = \{0, 1\}$ is on top of the representations \mathbf{r} . We further define the *advantage* of any MIA with respect to the data distribution \mathcal{D} as:

$$\text{Adv}_{\mathcal{D}}(\mathcal{A}_{MIA}) = \max_{A_{MIA} \in \mathcal{A}_{MIA}} |\Pr(A_{MIA}(\mathbf{r}) = a|u = a) - \Pr(A_{MIA}(\mathbf{r}) = a|u = 1 - a)|, \forall a \in \{0, 1\}, \quad (33)$$

where $\text{Adv}_{\mathcal{D}}(\mathcal{A}_{MIA}) = 1$ means the strongest MIA can *completely* infer the privacy membership through the learnt representation. In contrast, an MIA obtains a *random guessing* MIA performance if $\text{Adv}_{\mathcal{D}}(\mathcal{A}_{MIA}) = 0$.

Theorem 4. *Let $\mathbf{r} = f(\mathbf{x})$ be the representation with a bounded norm R outputted by the encoder f by Equation (6) on \mathbf{x} with label y , u be \mathbf{x} 's membership. Assume the task classifier C is C_L -Lipschitz. Then the utility loss/risk induced by all MIAs \mathcal{A}_{MIA} is bounded as below:*

$$\text{Risk}_{MIA}(C \circ f) \geq \Delta_{y|u} - 2R \cdot C_L \cdot \text{Adv}_{\mathcal{D}}(\mathcal{A}_{MIA}), \quad (34)$$

where $\Delta_{y|u} = |\Pr(y = 1|u = 0) - \Pr(y = 1|u = 1)|$ is a (task-dependent) constant.

Remark. Theorem 4 states any learning task classifier using representations learnt by the encoder incurs a risk, at the cost of membership protection—The larger the advantage $\text{Adv}_{\mathcal{D}}(\mathcal{A}_{MIA})$, the smaller the lower bound risk, and vice versa. Note that the lower bound is independent of the adversary. Hence, Theorem 4 reflects an inherent trade-off between utility preservation and membership protection.

B.2 Tradeoff of Inf^2 Guard against PIAs

Let \mathcal{A}_{PIA} be the set of all PIAs that have access to the representations \mathbf{R} of a dataset $\mathbf{X} = \{\mathbf{x}_i\}$ sampled from the data distribution \mathcal{D} , i.e., $\mathcal{A}_{PIA} = \{A_{PIA} : \mathbf{R} = f(\mathbf{X}) \in \mathcal{Z} \rightarrow u \in \{0, 1\}\}$. Let the dataset representation space is bounded, i.e., $\max_{\mathbf{R} \in \mathcal{Z}} \|\mathbf{R}\| \leq R$. We further define the advantage of any PIA with respect to the data distribution \mathcal{D} as:

$$\text{Adv}_{\mathcal{D}}(\mathcal{A}_{PIA}) = \max_{A_{PIA} \in \mathcal{A}_{PIA}} |\Pr(A_{PIA}(\mathbf{R}) = a|u = a) - \Pr(A_{PIA}(\mathbf{R}) = a|u = 1 - a)|, \forall a \in \{0, 1\}, \quad (35)$$

where $\text{Adv}_{\mathcal{D}}(\mathcal{A}_{PIA}) = 1$ means the strongest PIA can *completely* infer the privacy dataset property through the learnt dataset representations, while $\text{Adv}_{\mathcal{D}}(\mathcal{A}_{PIA}) = 0$ implies a *random guessing* PI performance.

Theorem 5. *Let (\mathbf{X}, \mathbf{y}) be a dataset randomly sampled from the data distribution \mathcal{D} and $\mathbf{R} = f(\mathbf{X})$ be the dataset representation outputted by the encoder f by Equation (11) on \mathbf{X} . Assume the representation space is bounded by R and task*

classifier C is C_L -Lipschitz. Let u be \mathbf{X} 's private property. Then, the risk induced by all PIAs \mathcal{A}_{PIA} is bounded as below:

$$\text{Risk}_{PIA}(C \circ f) \geq \Delta_{y|u} - 2R \cdot C_L \cdot \text{Adv}_{\mathcal{D}}(\mathcal{A}_{PIA}). \quad (36)$$

where $\Delta_{y|u}$ is same as in Equation 34.

Remark. Similarly, Theorem 5 states any learning task classifier using representations learnt by the encoder incurs a utility loss. The larger/smaller the advantage $\text{Adv}_{\mathcal{D}}(\mathcal{A}_{PIA})$, the smaller/larger the lower bound risk. Also, the lower bound is independent of the adversary, and thus covers the strongest PIA. Hence, Theorem 5 shows an inherent tradeoff between utility preservation and dataset property protection.

B.3 Tradeoff of Inf^2 Guard against DRAs

Let \mathcal{A}_{DRA} be the set of all DRAs that have access to the perturbed data representations, i.e., $\mathcal{A}_{DRA} = \{A_{DRA} : \mathbf{r} + \boldsymbol{\delta} \in \mathcal{Z} \times \mathcal{P} \rightarrow \mathbf{x} \in \mathcal{X}\}$. We assume the perturbed representation space \mathcal{Z} is bounded, i.e., $\max_{\mathbf{r} + \boldsymbol{\delta} \in \mathcal{Z} \times \mathcal{P}} \|\mathbf{r} + \boldsymbol{\delta}\| \leq R'$. We also denote the perturbed representation as $\mathbf{r}' = \mathbf{r} + \boldsymbol{\delta}$ for short. We further define the advantage¹⁰ of any DRA with respect to the data distribution \mathcal{D} as:

$$\text{Adv}_{\mathcal{D}}(\mathcal{A}_{DRA}) = \max_{A_{DRA} \in \mathcal{A}_{DRA}} |\Pr(A_{DRA}(\mathbf{r}') = \mathbf{x}|y = 0) - \Pr(A_{DRA}(\mathbf{r}') = \mathbf{x}|y = 1)|, \quad (37)$$

where $\text{Adv}_{\mathcal{D}}(\mathcal{A}_{DRA}) = 1$ means the strongest DRA can *completely* reconstruct the private data through the perturbed representation. In contrast, $\text{Adv}_{\mathcal{D}}(\mathcal{A}_{DRA}) = 0$ means the adversary cannot infer any raw data information.

Theorem 6. *Let f and \mathbf{r}' be the learnt encoder and perturbed representation with a bounded norm R' outputted by Equation (20) on \mathbf{x} with label y , respectively. Assume the task classifier C is C_L -Lipschitz. Then the utility loss induced by all DR adversaries \mathcal{A}_{DRA} is bounded as below:*

$$\text{Risk}_{DRA}(C \circ f) \geq \Delta_y - 2R' \cdot C_L \cdot \text{Adv}_{\mathcal{D}}(\mathcal{A}_{DRA}), \quad (38)$$

where $\Delta_y = |\Pr(y = 1) - \Pr(y = 0)|$ is a constant.

Remark. Theorem 6 states that, given a task-dependent constant Δ_y , any learning task classifier using representations learnt by the encoder f incurs a risk. The larger the advantage $\text{Adv}_{\mathcal{D}}(\mathcal{A}_{DRA})$, the smaller the lower bound risk, and vice versa. Note that the lower bound covers the strongest DRA. Hence, Theorem 6 reflects an inherent trade-off between utility preservation and data sample protection.

B.4 Proof of Theorem 4 for MIAs

We first introduce the following definitions and lemmas.

Definition 1 (Lipschitz function and Lipschitz norm). *A function $f : A \rightarrow \mathbb{R}^m$ is L -Lipschitz continuous, if for any $a, b \in A$, $\|f(a) - f(b)\| \leq L \cdot \|a - b\|$. Lipschitz norm of f , i.e., $\|f\|_L$, is defined as $\|f\|_L = \max \frac{\|f(a) - f(b)\|_L}{\|a - b\|_L}$.*

¹⁰Note that our defined advantage is different from that in [56].

Definition 2 (Total variance (TV) distance). Let \mathcal{D}_1 and \mathcal{D}_2 be two distributions over the same sample space Γ , the TV distance between \mathcal{D}_1 and \mathcal{D}_2 is defined as: $d_{TV}(\mathcal{D}_1, \mathcal{D}_2) = \max_{E \subseteq \Gamma} |\mathcal{D}_1(E) - \mathcal{D}_2(E)|$.

Definition 3 (1-Wasserstein distance). Let \mathcal{D}_1 and \mathcal{D}_2 be two distributions over the same sample space Γ , the 1-Wasserstein distance between \mathcal{D}_1 and \mathcal{D}_2 is defined as $W_1(\mathcal{D}_1, \mathcal{D}_2) = \max_{\|f\|_L \leq 1} |\int_{\Gamma} f d\mathcal{D}_1 - \int_{\Gamma} f d\mathcal{D}_2|$, where $\|\cdot\|_L$ is the Lipschitz norm of a real-valued function.

Definition 4 (Pushforward distribution). Let \mathcal{D} be a distribution over a sample space and g be a function of the same space. Then we call $g(\mathcal{D})$ the induced pushforward distribution of \mathcal{D} .

Lemma 4 (Contraction of the 1-Wasserstein distance). Let g be a function defined on a space and C_L be the constant such that $\|g\|_L \leq C_L$. Then for any two distributions \mathcal{D}_1 and \mathcal{D}_2 over this space, $W_1(g(\mathcal{D}_1), g(\mathcal{D}_2)) \leq C_L \cdot W_1(\mathcal{D}_1, \mathcal{D}_2)$.

Lemma 5 (1-Wasserstein distance over two Bernoulli random scalars). Let y_1 and y_2 be two Bernoulli random scalars with distributions \mathcal{D}_1 and \mathcal{D}_2 , respectively. Then, $W_1(\mathcal{D}_1, \mathcal{D}_2) = |\Pr(y_1 = 1) - \Pr(y_2 = 1)|$.

Lemma 6 (Relationship between the 1-Wasserstein distance and the TV distance [25]). Let g be a function defined on a norm-bounded space \mathcal{Z} , where $\max_{\mathbf{r} \in \mathcal{Z}} \|\mathbf{r}\| \leq R$, and \mathcal{D}_1 and \mathcal{D}_2 are two distributions over the space \mathcal{Z} . Then $W_1(g(\mathcal{D}_1), g(\mathcal{D}_2)) \leq 2R \cdot d_{TV}(g(\mathcal{D}_1), g(\mathcal{D}_2))$.

We now prove Theorem 4.

Proof. We denote $\mathcal{D}_{\mathbf{x}|u}$ as the conditional data distribution of \mathcal{D} given u , i.e., $\mathbf{x}|u \sim \mathcal{D}_{\mathbf{x}|u}$, and $\mathcal{D}_{y|u}$ as the conditional label distribution given u , i.e., $y|u \sim \mathcal{D}_{y|u}$. As C is a binary task classifier on top of the encoder f , it follows that the pushforward $C \circ f(\mathcal{D}_{\mathbf{x}|u=0})$ and $C \circ f(\mathcal{D}_{\mathbf{x}|u=1})$ induce two distributions over $\{0, 1\}$. We denote Cf as $C \circ f$ for short. By leveraging the triangle inequalities of 1-Wasserstein distance, we have

$$W_1(\mathcal{D}_{y|u=0}, \mathcal{D}_{y|u=1}) \leq W_1(\mathcal{D}_{y|u=0}, Cf(\mathcal{D}_{\mathbf{x}|u=0})) + W_1(Cf(\mathcal{D}_{\mathbf{x}|u=0}), Cf(\mathcal{D}_{\mathbf{x}|u=1})) + W_1(Cf(\mathcal{D}_{\mathbf{x}|u=1}), \mathcal{D}_{y|u=1}) \quad (39)$$

Using Lemma 5 on Bernoulli r.v. $y|u = a$, we have

$$W_1(\mathcal{D}_{y|u=0}, \mathcal{D}_{y|u=1}) = |\Pr_{\mathcal{D}}(y = 1|u = 0) - \Pr_{\mathcal{D}}(y = 1|u = 1)| = \Delta_{y|u}. \quad (40)$$

Using Lemma 4 on the contraction of the 1-Wasserstein distance and that $\|C\|_L \leq C_L$, we have

$$W_1(Cf(\mathcal{D}_{\mathbf{x}|u=0}), Cf(\mathcal{D}_{\mathbf{x}|u=1})) \leq C_L \cdot W_1(f(\mathcal{D}_{\mathbf{x}|u=0}), f(\mathcal{D}_{\mathbf{x}|u=1})). \quad (41)$$

Using Lemma 6 with $\max_{\mathbf{r}} \|\mathbf{r}\| \leq R$, we have

$$W_1(f(\mathcal{D}_{\mathbf{x}|u=0}), f(\mathcal{D}_{\mathbf{x}|u=1})) \leq 2R \cdot d_{TV}(f(\mathcal{D}_{\mathbf{x}|u=0}), f(\mathcal{D}_{\mathbf{x}|u=1})). \quad (42)$$

We next show $d_{TV}(f(\mathcal{D}_{\mathbf{x}|u=0}), f(\mathcal{D}_{\mathbf{x}|u=1})) = \text{Adv}_{\mathcal{D}}(\mathcal{A}_{MIA})$.

$$\begin{aligned} d_{TV}(f(\mathcal{D}_{\mathbf{x}|u=0}), f(\mathcal{D}_{\mathbf{x}|u=1})) &= \max_E |\Pr_{f(\mathcal{D}_{\mathbf{x}|u=0})}(E) - \Pr_{f(\mathcal{D}_{\mathbf{x}|u=1})}(E)| \\ &= \max_{A_E \in \mathcal{A}_{MIA}} |\Pr_{\mathbf{r} \sim f(\mathcal{D}_{\mathbf{x}|u=0})}(A_E(\mathbf{r}) = 1) - \Pr_{\mathbf{r} \sim f(\mathcal{D}_{\mathbf{x}|u=1})}(A_E(\mathbf{r}) = 1)| \\ &= \max_{A_E \in \mathcal{A}_{MIA}} |\Pr(A_E(\mathbf{r}) = 1|u = 0) - \Pr(A_E(\mathbf{r}) = 1|u = 1)| \\ &= \text{Adv}_{\mathcal{D}}(\mathcal{A}_{MIA}), \end{aligned} \quad (43)$$

where the first equation uses the definition of TV distance, and $A_E(\cdot)$ is the characteristic function of the event E in the second equation. With Equations 41-43, we have

$$W_1(Cf(\mathcal{D}_{\mathbf{x}|u=0}), Cf(\mathcal{D}_{\mathbf{x}|u=1})) \leq 2R \cdot C_L \cdot \text{Adv}_{\mathcal{D}}(\mathcal{A}_{MIA}). \quad (44)$$

Furthermore, using Lemma 5 on Bernoulli random variables y and $Cf(\mathbf{x})$, we have

$$\begin{aligned} W_1(\mathcal{D}_{y|u=a}, Cf(\mathcal{D}_{\mathbf{x}|u=a})) &= |\Pr_{\mathcal{D}}(y = 1|u = a) - \Pr_{\mathcal{D}}(Cf(\mathbf{x}) = 1|u = a)| \\ &= |\mathbb{E}_{\mathcal{D}}[y|u = a] - \mathbb{E}_{\mathcal{D}}[Cf(\mathbf{x})|u = a]| \\ &\leq \mathbb{E}_{\mathcal{D}}[|y - Cf(\mathbf{x})||u = a] = \Pr_{\mathcal{D}}(y \neq Cf(\mathbf{x})|u = a) \end{aligned} \quad (45)$$

Finally, by combining Equations 39-45, we have:

$$\begin{aligned} \Delta_{y|u} &\leq \Pr_{\mathcal{D}}(y \neq Cf(\mathbf{x})|u = 0) + \Pr_{\mathcal{D}}(y \neq Cf(\mathbf{x})|u = 1) \\ &\quad + 2R \cdot C_L \cdot \text{Adv}_{\mathcal{D}}(\mathcal{A}_{MIA}). \end{aligned} \quad (46)$$

Hence, $\text{Risk}_{MI}(C \circ f) = \Pr_{\mathcal{D}}(y \neq Cf(\mathbf{x})|u = 0) + \Pr_{\mathcal{D}}(y \neq Cf(\mathbf{x})|u = 1) \geq \Delta_{y|u} - 2R \cdot C_L \cdot \text{Adv}_{\mathcal{D}}(\mathcal{A}_{MIA})$. \square

B.5 Proof of Theorem 5 for PIAs

Proof. We follow the similar strategy for proving Theorem 4. To differential the conditional *data sample* distribution $\mathcal{D}_{\mathbf{x}|u}$ in MIAs, we denote $\mathcal{D}_{\mathbf{X}|u}$ as the conditional *dataset* distribution of \mathcal{D} given the dataset property u , and $\mathcal{D}_{\mathbf{y}|u}$ as the conditional distribution of dataset labels \mathbf{y} given u . Also, the pushforward $Cf(\mathcal{D}_{\mathbf{X}|u=0})$ and $Cf(\mathcal{D}_{\mathbf{X}|u=1})$ induce two distributions over $\{0, 1\}^{|\mathbf{y}|}$. First, by leveraging the triangle inequalities of the 1-Wasserstein distance, we have

$$\begin{aligned} W_1(\mathcal{D}_{\mathbf{y}|u=0}, \mathcal{D}_{\mathbf{y}|u=1}) &\leq W_1(\mathcal{D}_{\mathbf{y}|u=0}, Cf(\mathcal{D}_{\mathbf{X}|u=0})) \\ &\quad + W_1(Cf(\mathcal{D}_{\mathbf{X}|u=0}), Cf(\mathcal{D}_{\mathbf{X}|u=1})) + W_1(Cf(\mathcal{D}_{\mathbf{X}|u=1}), \mathcal{D}_{\mathbf{y}|u=1}) \end{aligned} \quad (47)$$

Using Lemma 5 on Bernoulli random variables $y_i|u = a$ and that $y_i \in \mathbf{y}$ are independent, we have

$$\begin{aligned} W_1(\mathcal{D}_{\mathbf{y}|u=0}, \mathcal{D}_{\mathbf{y}|u=1}) &= \frac{1}{|\mathbf{y}|} \sum_{y_i \in \mathbf{y}} W_1(\mathcal{D}_{y_i|u=0}, \mathcal{D}_{y_i|u=1}) \\ &= \frac{1}{|\mathbf{y}|} \sum_{y_i \in \mathbf{y}} |\Pr_{\mathcal{D}}(y_i = 1|u = 0) - \Pr_{\mathcal{D}}(y_i = 1|u = 1)| \\ &= |\Pr_{\mathcal{D}}(y = 1|u = 0) - \Pr_{\mathcal{D}}(y = 1|u = 1)| \\ &= \Delta_{y|u}, \end{aligned} \quad (48)$$

where in the first equality and third equality we use the independence of $\{y_i\}$'s and second equality uses Equation 40.

Using Lemma 4 on the contraction of the 1-Wasserstein distance and that $\|c\|_L \leq C_L$, we have

$$W_1(Cf(\mathcal{D}_{\mathbf{X}|u=0}), Cf(\mathcal{D}_{\mathbf{X}|u=1})) \leq C_L \cdot W_1(f(\mathcal{D}_{\mathbf{X}|u=0}), f(\mathcal{D}_{\mathbf{X}|u=1})). \quad (49)$$

Using Lemma 6 with $\max_{\mathbf{R}} \|\mathbf{R}\| \leq R$, we have

$$W_1(f(\mathcal{D}_{\mathbf{X}|u=0}), f(\mathcal{D}_{\mathbf{X}|u=1})) \leq 2R \cdot d_{TV}(f(\mathcal{D}_{\mathbf{X}|u=0}), f(\mathcal{D}_{\mathbf{X}|u=1})).$$

We next show $d_{TV}(f(\mathcal{D}_{\mathbf{X}|u=0}), f(\mathcal{D}_{\mathbf{X}|u=1})) = \text{Adv}_{\mathcal{D}}(\mathcal{A}_{PIA})$.

$$\begin{aligned} d_{TV}(f(\mathcal{D}_{\mathbf{X}|u=0}), f(\mathcal{D}_{\mathbf{X}|u=1})) &= \max_E |\Pr_{f(\mathcal{D}_{\mathbf{X}|u=0})}(E) - \Pr_{f(\mathcal{D}_{\mathbf{X}|u=1})}(E)| \\ &= \max_{A_E \in \mathcal{A}_{PIA}} |\Pr_{\mathbf{R} \sim f(\mathcal{D}_{\mathbf{X}|u=0})}(A_E(\mathbf{R}) = 1) - \Pr_{\mathbf{R} \sim f(\mathcal{D}_{\mathbf{X}|u=1})}(A_E(\mathbf{R}) = 1)| \\ &= \max_{A_E \in \mathcal{A}_{PIA}} |\Pr(A_E(\mathbf{R}) = 1|u=0) - \Pr(A_E(\mathbf{R}) = 1|u=1)| \\ &= \text{Adv}_{\mathcal{D}}(\mathcal{A}_{PIA}). \end{aligned} \quad (50)$$

With Equations 49-50, we thus have

$$W_1(Cf(\mathcal{D}_{\mathbf{X}|u=0}), Cf(\mathcal{D}_{\mathbf{X}|u=1})) \leq 2R \cdot C_L \cdot \text{Adv}_{\mathcal{D}}(\mathcal{A}_{PIA}).$$

Further, as $\{y_i\}$'s are independent and using Lemma 5 on Bernoulli random variables y_i and $Cf(\mathbf{x}_i)$, we have

$$\begin{aligned} W_1(\mathcal{D}_{\mathbf{y}|u=a}, Cf(\mathcal{D}_{\mathbf{X}|u=a})) &= \frac{1}{|\mathbf{y}|} \sum_{(\mathbf{x}_i, y_i) \in (\mathbf{X}, \mathbf{y})} W_1(\mathcal{D}_{y_i|u=a}, Cf(\mathcal{D}_{\mathbf{x}_i|u})) \\ &= \frac{1}{|\mathbf{y}|} \sum_{(\mathbf{x}_i, y_i) \in (\mathbf{X}, \mathbf{y})} |\Pr_{\mathcal{D}}(y_i = 1|u=a) - \Pr_{\mathcal{D}}(Cf(\mathbf{x}_i) = 1|u=a)| \\ &= \frac{1}{|\mathbf{y}|} \sum_{(\mathbf{x}_i, y_i) \in (\mathbf{X}, \mathbf{y})} |\mathbb{E}_{\mathcal{D}}[y_i|u=a] - \mathbb{E}_{\mathcal{D}}[Cf(\mathbf{x}_i)|u=a]| \\ &\leq \frac{1}{|\mathbf{y}|} \sum_{(\mathbf{x}_i, y_i) \in (\mathbf{X}, \mathbf{y})} \mathbb{E}_{\mathcal{D}}[|y_i - Cf(\mathbf{x}_i)||u=a] \\ &= \frac{1}{|\mathbf{y}|} \sum_{(\mathbf{x}_i, y_i) \in (\mathbf{X}, \mathbf{y})} \Pr_{\mathcal{D}}(y_i \neq Cf(\mathbf{x}_i)|u=a), \end{aligned} \quad (51)$$

where again the first equality uses independence of $\{y_i\}$'s.

Finally, by combining Equations 47-51,

$$\begin{aligned} \Delta_{\mathbf{y}|u} &\leq \frac{1}{|\mathbf{y}|} \sum_{(\mathbf{x}_i, y_i) \in (\mathbf{X}, \mathbf{y})} \Pr_{\mathcal{D}}(y_i \neq Cf(\mathbf{x}_i)|u=0) \\ &\quad + \frac{1}{|\mathbf{y}|} \sum_{(\mathbf{x}_i, y_i) \in (\mathbf{X}, \mathbf{y})} \Pr_{\mathcal{D}}(y_i \neq Cf(\mathbf{x}_i)|u=1) \\ &\quad + 2R \cdot C_L \cdot \text{Adv}_{\mathcal{D}}(\mathcal{A}_{PIA}). \end{aligned} \quad (52)$$

Hence, $\text{Risk}_{PI}(C \circ f) = \frac{1}{|\mathbf{y}|} \sum_{(\mathbf{x}_i, y_i) \in (\mathbf{X}, \mathbf{y})} \Pr_{\mathcal{D}}(y_i \neq Cf(\mathbf{x}_i)) \geq \Delta_{\mathbf{y}|u} - 2R \cdot C_L \cdot \text{Adv}_{\mathcal{D}}(\mathcal{A}_{PIA})$. \square

B.6 Proof of Theorem 6 for DRAs

Proof. We denote $\mathcal{D}_{\mathbf{x}|y}$ as the conditional data sample distribution of \mathcal{D} given y and $\mathcal{P}_{\boldsymbol{\delta}}$ as the perturbation distribution on $\boldsymbol{\delta}$. We further denote $\mathcal{D}_{\mathbf{x}|y} \oplus \mathcal{P}_{\boldsymbol{\delta}}$ as the combined distribution

of the two. Accordingly, $\mathbf{r}' = \mathbf{r} + \boldsymbol{\delta}$ is sampled from this combined distribution. By leveraging the triangle inequalities of the 1-Wasserstein distance, we have

$$\begin{aligned} W_1(\mathcal{D}_{y=0|\mathbf{x}}, \mathcal{D}_{y=1|\mathbf{x}}) &\leq W_1(\mathcal{D}_{y=0|\mathbf{x}}, Cf(\mathcal{D}_{\mathbf{x}|y=0} \oplus \mathcal{P}_{\boldsymbol{\delta}})) \\ &\quad + W_1(Cf(\mathcal{D}_{\mathbf{x}|y=0} \oplus \mathcal{P}_{\boldsymbol{\delta}}), Cf(\mathcal{D}_{\mathbf{x}|y=1} \oplus \mathcal{P}_{\boldsymbol{\delta}})) \\ &\quad + W_1(Cf(\mathcal{D}_{\mathbf{x}|y=1} \oplus \mathcal{P}_{\boldsymbol{\delta}}), \mathcal{D}_{y=1|\mathbf{x}}). \end{aligned} \quad (53)$$

Using Lemma 5 on Bernoulli r.v. y , we have

$$W_1(\mathcal{D}_{y=0|\mathbf{x}}, \mathcal{D}_{y=1|\mathbf{x}}) = |\Pr_{\mathcal{D}}(y=0) - \Pr_{\mathcal{D}}(y=1)| = \Delta_{\mathbf{y}}. \quad (54)$$

Using Lemma 4 on the contraction of the 1-Wasserstein distance and that $\|C\|_L \leq C_L$, we have

$$\begin{aligned} W_1(Cf(\mathcal{D}_{\mathbf{x}|y=0} \oplus \mathcal{P}_{\boldsymbol{\delta}}), Cf(\mathcal{D}_{\mathbf{x}|y=1} \oplus \mathcal{P}_{\boldsymbol{\delta}})) \\ \leq C_L \cdot W_1(f(\mathcal{D}_{\mathbf{x}|y=0} \oplus \mathcal{P}_{\boldsymbol{\delta}}), f(\mathcal{D}_{\mathbf{x}|y=1} \oplus \mathcal{P}_{\boldsymbol{\delta}})). \end{aligned} \quad (55)$$

Using Lemma 6 with $\max_{\mathbf{r}'} \|\mathbf{r}'\| \leq R'$, we have

$$\begin{aligned} W_1(f(\mathcal{D}_{\mathbf{x}|y=0} \oplus \mathcal{P}_{\boldsymbol{\delta}}), f(\mathcal{D}_{\mathbf{x}|y=1} \oplus \mathcal{P}_{\boldsymbol{\delta}})) \\ \leq 2R' \cdot d_{TV}(f(\mathcal{D}_{\mathbf{x}|y=0} \oplus \mathcal{P}_{\boldsymbol{\delta}}), f(\mathcal{D}_{\mathbf{x}|y=1} \oplus \mathcal{P}_{\boldsymbol{\delta}})). \end{aligned} \quad (56)$$

We further show that $d_{TV}(f(\mathcal{D}_{\mathbf{x}|y=0} \oplus \mathcal{P}_{\boldsymbol{\delta}}), f(\mathcal{D}_{\mathbf{x}|y=1} \oplus \mathcal{P}_{\boldsymbol{\delta}})) = \text{Adv}_{\mathcal{D}}(\mathcal{A}_{DRA})$. Specifically,

$$\begin{aligned} d_{TV}(f(\mathcal{D}_{\mathbf{x}|y=0} \oplus \mathcal{P}_{\boldsymbol{\delta}}), f(\mathcal{D}_{\mathbf{x}|y=1} \oplus \mathcal{P}_{\boldsymbol{\delta}})) &= \max_E |\Pr_{f(\mathcal{D}_{\mathbf{x}|y=0} \oplus \mathcal{P}_{\boldsymbol{\delta}})}(E) - \Pr_{f(\mathcal{D}_{\mathbf{x}|y=1} \oplus \mathcal{P}_{\boldsymbol{\delta}})}(E)| \\ &= \max_{A_E \in \mathcal{A}_{DRA}} |\Pr_{\mathbf{r}' \sim f(\mathcal{D}_{\mathbf{x}|y=0} \oplus \mathcal{P}_{\boldsymbol{\delta}})}(A_E(\mathbf{r}') = \mathbf{x}) - \Pr_{\mathbf{r}' \sim f(\mathcal{D}_{\mathbf{x}|y=1} \oplus \mathcal{P}_{\boldsymbol{\delta}})}(A_E(\mathbf{r}') = \mathbf{x})| \\ &= \max_{A_E \in \mathcal{A}_{DRA}} |\Pr(A_E(\mathbf{r}') = \mathbf{x}|y=0) - \Pr(A_E(\mathbf{r}') = \mathbf{x}|y=1)| \\ &= \text{Adv}_{\mathcal{D}}(\mathcal{A}_{DRA}), \end{aligned} \quad (57)$$

where the first equation uses the definition of TV distance, and $A_E(\cdot)$ is the characteristic function of the event E in the second equation. With Equations 55-57, we have

$$W_1(Cf(\mathcal{D}_{\mathbf{x}|y=0} \oplus \mathcal{P}_{\boldsymbol{\delta}}), Cf(\mathcal{D}_{\mathbf{x}|y=1} \oplus \mathcal{P}_{\boldsymbol{\delta}})) \leq 2R' \cdot C_L \cdot \text{Adv}_{\mathcal{D}}(\mathcal{A}_{DRA}).$$

Furthermore, using Lemma 5 on Bernoulli r.v.s y and $Cf(\mathbf{x})$:

$$\begin{aligned} W_1(\mathcal{D}_{y=1|\mathbf{x}}, Cf(\mathcal{D}_{\mathbf{x}|y=1} \oplus \mathcal{P}_{\boldsymbol{\delta}})) &= |\Pr_{\mathcal{D}}(y=1) - \Pr_{\mathcal{D} \times \mathcal{P}}(C(f(\mathbf{x}) + \boldsymbol{\delta}) = 1|y=1)| \\ &= |\mathbb{E}_{\mathcal{D}}[y] - \mathbb{E}_{\mathcal{D} \times \mathcal{P}}[C(f(\mathbf{x}) + \boldsymbol{\delta})|y=1]| \\ &\leq \mathbb{E}_{\mathcal{D} \times \mathcal{P}}[|y - C(f(\mathbf{x}) + \boldsymbol{\delta})|y=1]| \\ &= \Pr_{\mathcal{D} \times \mathcal{P}}(y \neq C(f(\mathbf{x}) + \boldsymbol{\delta})|y=1). \end{aligned} \quad (58)$$

Similarly,

$$W_1(\mathcal{D}_{y=0|\mathbf{x}}, Cf(\mathcal{D}_{\mathbf{x}|y=0} \oplus \mathcal{P}_{\boldsymbol{\delta}})) \leq \Pr_{\mathcal{D} \times \mathcal{P}}(y \neq C(f(\mathbf{x}) + \boldsymbol{\delta})|y=0). \quad (59)$$

Finally, by combining Equation 53-Equation 59,

$$\begin{aligned} \Delta_{\mathbf{y}} &\leq \Pr_{\mathcal{D} \times \mathcal{P}}(y \neq C(f(\mathbf{x}) + \boldsymbol{\delta})|y=1) + 2R' \cdot C_L \cdot \text{Adv}_{\mathcal{D}}(\mathcal{A}_{DRA}) \\ &\quad + \Pr_{\mathcal{D} \times \mathcal{P}}(y \neq C(f(\mathbf{x}) + \boldsymbol{\delta})|y=0) \end{aligned} \quad (60)$$

Hence, $\text{Risk}_{DR}(C \circ f) = \Pr_{\mathcal{D} \times \mathcal{P}}(y \neq C(f(\mathbf{x}) + \boldsymbol{\delta})|y=1) + \Pr_{\mathcal{D} \times \mathcal{P}}(y \neq C(f(\mathbf{x}) + \boldsymbol{\delta})|y=0) \geq \Delta_{\mathbf{y}} - 2R' \cdot C_L \cdot \text{Adv}_{\mathcal{D}}(\mathcal{A}_{DRA})$. \square

C Datasets and Network Architectures

C.1 Detailed Dataset Description

CIFAR-10 [40]. It contains 60,000 colored images of 32x32 resolution. The dataset consists of images belonging to 10 classes: airplane, automobile, bird, cat, deer, dog, frog, horse, ship and truck. There are 6,000 images per class. In this dataset, the primary task is to predict the label of the image.

Purchase100 [48]. The dataset includes 197,324 shopping records, where each data record corresponds to one customer and has 600 binary features (each corresponding to one item). Each feature reflects if the item is purchased by the customer or not. The data is clustered into 100 classes and the task is to predict the class for each customer.

Texas100 [61]. This dataset includes hospital discharge data published by the Texas Department of State Health Services. Data records have features about the external causes of injury (e.g., suicide, drug misuse), the diagnosis (e.g., schizophrenia, illegal abortion), the procedures the patient underwent (e.g., surgery), and generic information such as gender, age, race, hospital ID, and length of stay. The dataset contains 67,330 records and 6,170 binary features which represent the 100 most frequent medical procedures. The records are clustered into 100 classes, each representing a type of patient.

Census [66]. It consists of several categorical and numerical attributes like age, race, education level to predict whether a person makes over \$50K a year. We focus on the ratios of females (sex) as property.

RSNA Bone Age [66]. It contains X-Ray images of hands, with the task being predicting the patients’ age in months. We convert the task to binary classification based on an age threshold, 132 months, as a binary primary task. We focus on the ratios of the females (available as metadata) as properties.

CelebA [43]. It is a large-scale wild face attributes dataset that consists of 200,000 RGB celebrity images. Each image has 40 annotated binary attributes such as “gender”, “race”. We focus on smile detection as a primary task and the ratios of females (sex) as the private property.

CIFAR100 [40]. This dataset has 100 classes containing 600 colored images each, with size 32x32. There are 500 training images and 100 testing images per class. The learning task is classifying the 100 classes.

Activity [54]. This dataset contains data collected from smartphones carried by a person while performing 1 of 6 activities. There is a total of 516 features in a single row format. All features are pre-normalized and bounded by [-1, 1]. The data collected include statistical summaries of sensory data collected by the phone, including acceleration, orientation, etc.

C.2 More Experimental Setup

Training and testing: Table 9-Table 11 show the utility training/test and attack training/test sets.

Table 9: Training and test sets for primary and MIA tasks.

	CIFAR10	Purchase100	Texas100
Utility training set	25,000	98,662	33,665
Utility test set	25,000	98,662	33,665
Attack training set	40,000	157,859	53,864
Attack test set	10,000	39,465	13,466

Table 10: Training and test sets for primary and PIA tasks.

	Census	RSNA	CelebA
Subset size	[2,32k]	[2,100]	[2,20]
female ratios	{0.2, 0.3, ..., 0.5}	{0.2, 0.3, ..., 0.8}	{0.0, 0.1, ..., 1.0}
Attack train set	8k subsets	14k subsets	22k subsets
Attack test set	2k subsets	3.5k subsets	5.5k subsets
Utility train set	data in 8k subsets	in 14k subsets	in 22k subsets
Utility test set	data in 2k subsets	in 3.5k subsets	in 5.5k subsets

Table 11: Training and test sets for primary and DRA tasks.

	CIFAR10	CIFAR100	Activity
Utility/Attack training set	50,000	50,000	7,352
Utility test set	10,000	10,000	2,947
Attack test set	50	50	50

Differential Privacy (DP) against MIAs: DP provides an upper bound on the success of any MIA. We can add noise in several ways (e.g., to input data, model parameters, gradients, latent features, output scores) to ensure DP. Note that there exists an inherent trade-off between utility and privacy: a larger added noise often leads to a higher level of privacy protection, but incurs a larger utility loss. Here, we propose to use the below two ways.

- **DP-SGD** [3]: 1) *DP-SGD training*: It clips gradients (with a gradient norm bound) and adds Gaussian noise to the gradient in each SGD round when training the ML model (i.e., encoder + utility network). More details can be seen in Algorithm 1 in [3]. After training, the model ensures DP guarantees and the encoder is published. 2) *Attack training*: The attacker obtains the representations of the attack training data via querying the trained encoder and uses these representations to train the MIA classifier. 3) *Defense/attack testing*: The utility test set is used to obtain the utility via querying the trained ML model; and the attack test set to obtain the MIA accuracy via querying the trained encoder and trained MIA classifier.

We used the Opacus library (<https://opacus.ai/>), a Py-Torch extension that enables training models with DP-SGD and dynamically tracks privacy budget and utility. In the experiments, we tried ϵ in DP-SGD from 0.5 to 16.

- **DP-encoder**: 1) *Normal training*: It first trains the encoder + utility network using the (utility) training set. The encoder is then frozen and can be used to produce data representations when queried by data samples. 2) *Defense via adding noise to the representations*: We add Gaussian noise (i.e., $\mathcal{N}(0, \sigma^2)$) to the representations by querying the encoder with the attack training data to produce the noisy representations. Notice that, since the Gaussian noises are injected to

Table 12: Network architectures for the used datasets (MIAs)

Encoder	Membership Network	Utility Network
CIFAR10		
conv3-64 (ResNet Block 6) BN-64 MaxPool	2xconv3-512 (ResNet Block 6) avgpool & Flatten	2xconv3-512 avgpool & Flatten
2xconv3-64 (ResNet Block)	Linear-512	Linear-512
2xconv3-64 (ResNet Block)	Linear-2 classes	Linear-#labels
3xconv3-64 (CustomBlock)		
2xconv3-128 (ResNet Block)		
2xconv3-128 (ResNet Block)		
3xconv3-128 (CustomBlock)		
2xconv3-256 (ResNet Block)		
conv3-512 (ResNet Block)		
Purchase100		
Linear-600 & Tanh	Linear-1024 & ReLU	Linear-128 & ReLU
Linear-512 & Tanh	Linear-512 & ReLU	Linear-256 & ReLU
Linear-256 & Tanh	Linear-256 & Tanh	Linear-128
	Linear-128 & Tanh	3xLinear-256
	Linear-2 classes	Linear-#labels
Texas 100		
Linear-6169 & ReLU	Linear-128 & ReLU	Linear-128
Linear-1024 & ReLU	Linear-256 & ReLU	Linear-#labels
Linear-2048 & ReLU	Linear-128 & ReLU	
Linear-1024 & ReLU	Linear-128	
Linear-512 & ReLU	Linear-2 classes	
Linear-256 & ReLU		
Linear-128 & ReLU		

the matrix-outputs (data representations), if needed, the actual DP guarantee (i.e., privacy bounds) can be derived via Rényi Differential Privacy [46], similar to the theoretical studies in [47, 68]. We skip the details here since this work does not focus on the derivation for the privacy bounds of DP-encoder. 3) *Attack training*: The attacker uses the noisy representations of attack training data to train the MIA classifier. 4) *Defense/attack testing*: We use the utility test set to obtain the utility via querying the trained encoder and utility network; and use the attack test set to obtain the MIA accuracy on the trained encoder and trained MIA classifier. We call this *DP-encoder* as we add noise to the representations outputted by the well-trained encoder.

DP-encoder against PIAs: We follow the strategy in DP against MIAs and choose the DP-encoder, as DP-SGD is ineffective in this setting [66]. The only difference is that we now add Gaussian noise to the mean-aggregated representation of a subset, instead of the individual representation.

Data reconstruction attack/defense on shallow encoder: As shown in [30], when the encoder is deep, it is difficult for the attacker to reconstruct the input data from the representation. To ensure DRAs be effective, we use a shallow 2-layer encoder. As a result, this makes the defense more challenging.

C.3 Network Architectures

Network architectures for the neural networks used in defense training are detailed in Table 12-Table 14.

Table 13: Network architectures for the used datasets (PIAs). BN: BatchNorm, SC: Shortcut Connection

Encoder	Property Network	Utility Network
RSNA Bone Age		
conv2-64 & BN-64 ReLU & MaxPool	Linear-1024 ReLU	conv2d-1024 ReLU
DenseBlock-64 TransitionLayer-64	Linear-512 ReLU	AdaptiveAvgPool2d
DenseBlock-128 TransitionLayer-128	Linear-256 ReLU	Linear-#labels
DenseBlock-256 TransitionLayer-256	Linear-128 ReLU	
DenseBlock-512 AdaptiveAvgPool	Linear-#property values	
Census		
conv1d-256 & ReLU conv1d-128 & ReLU	Linear-128 & ReLU Linear-64 & ReLU	Conv1d-64 & ReLU Conv1d-32 & ReLU
AdaptiveMaxPool1d-1 Linear-128	Linear-#property values	AdaptiveAvgPool1d-1
AdaptiveMaxPool1d-1		Linear-#labels
CelebA		
conv3-64 & BN-64 ReLU & MaxPool	FCResidualBlock (512->256)	Linear-512
Residual Block 1 & 2 conv3-64 & BN-64 ReLU & conv3-64 BN-64 & SC & ReLU	FCResidualBlock (256->128)	Linear-#labels
Residual Block 3 & 4 conv3-128 & BN-128 ReLU & conv3-128 BN-128 & SC & ReLU	Linear-128	
Residual Block 5 & 6 conv3-256 & BN-256 ReLU & conv3-256 BN-256 & SC & ReLU	Linear-#property values	
Residual Block 7 & 8 conv3-512 & BN-512 ReLU & conv3-512 BN-512 & SC & ReLU		

Table 14: Network architectures for the used datasets (DRA)

Encoder	Reconstruction Network	Utility Network
CIFAR10 (CIFAR100)		
conv2-32 & BN-32 conv2-32 & BN-32	conv2-32 & BN-32	conv2-64 & BN-64 conv2-128 & BN-128 ReLU
		conv2-128 & BN-128 U ReLU
		conv2-128 & BN-128 ReLU
		conv2-128 & BN-128 ReLU
		conv2-64 & BN-64 ReLU
		Flatten
		Linear-1024 & BN-1024 ReLU
		Linear-64 (256) BN-64 (256) ReLU
		Linear-#labels
Activity		
Linear-256 BN-256 & ReLU	Linear-128 BN-128 & ReLU	Linear-32 BN-32 & ReLU
Linear-128 BN-128 & ReLU	Linear-32 BN-32 & ReLU	Linear-12 BN-12 & ReLU
Linear-32 BN-32 & ReLU		Linear-#labels

Table 15: Impact of the size of the encoder on Inf^2Guard defense results against MIAs (we fix the utility classifier and privacy protection/attack classifier). A larger encoder can have (marginally) better MIA performance without defense.

CIFAR10			
#parameters	λ	Utility	MIA Acc
Encoder: 4,898,112	0	77.83%	63.62%
Utility: 4,725,770	0.25	77.53%	56.2%
Pri/Atk: 4,721,153	0.5	77%	52.08%
	0.75	76%	50%
	1	10%	49.99%
Encoder: 6,448,192	0	80.88%	68.78%
Utility: 4,725,770	0.25	78.66%	55.39%
Pri/Atk: 4,721,153	0.5	77.80%	51.78%
	0.75	76.85%	50.31%
	1	13.44%	50%
Encoder: 7,018,944	0	78.85%	70.05%
Utility: 4,725,770	0.25	78.15%	55.88%
Pri/Atk: 4,721,153	0.5	78.00%	53.53%
	0.75	77.20%	51.08%
	1	20%	50%

Purchase100			
#parameters	λ	Utility	MIA Acc
Encoder: 471,936	0	80.08%	59.31%
Utility: 25,700	0.25	80.08%	51%
Pri/Atk: 66,049	0.5	80%	50%
	0.75	80%	50%
	1	20%	49.99%
Encoder: 734,592	0	81.65%	68.36%
Utility: 25,700	0.25	80.87%	60%
Pri/Atk: 66,049	0.5	80%	51%
	0.75	78%	50%
	1	20%	50%
Encoder: 1,304,448	0	80.65%	69.65%
Utility: 25,700	0.25	80.87%	61%
Pri/Atk: 66,049	0.5	80%	53%
	0.75	78%	50%
	1	20%	50%

Texas100			
#parameters	λ	Utility	MIA Acc
Encoder: 7,532,416	0	46.52%	68.96%
Utility: 25,700	0.25	46.20%	60%
Pri/Atk: 66,049	0.5	46%	50%
	0.75	46%	50%
	1	2%	50%
Encoder: 9,106,304	0	49.76%	70.21%
Utility: 25,700	0.25	49.05%	61%
Pri/Atk: 66,049	0.5	46%	50%
	0.75	46%	50%
	1	2%	50%
Encoder: 11,204,480	0	51.05%	69.10%
Utility: 25,700	0.25	51%	61%
Pri/Atk: 66,049	0.5	51%	50%
	0.75	46.82%	50%
	1	2%	50%

C.4 More Experimental Results

More results on defending against MIAs: Table 15 shows the Inf^2Guard results against MIAs, with varying sizes of the encoder. We can see a larger encoder can have (marginally) better MIA performance without defense. One possible is that

Table 16: More DP results against MIAs.

DP-SGD	CIFAR10		Purchase100		Texas100	
	Utility	MIA Acc	Utility	MIA Acc	Utility	MIA Acc
$\epsilon = 0.5$	46%	50%	40%	52%	11%	51%
$\epsilon = 1$	48%	51%	48%	54%	15%	52%
$\epsilon = 2$	59%	55%	53%	57%	26%	54%
$\epsilon = 4$	61%	57%	60%	59%	33%	55%
$\epsilon = 8$	65%	59%	71%	62%	39%	57%
$\epsilon = 16$	68%	62%	78%	66%	45%	59%

DP-encoder	CIFAR10		Purchase100		Texas100	
	Utility	MIA Acc	Utility	MIA Acc	Utility	MIA Acc
$\sigma^2 = 10$	48%	51%	32%	51%	10%	50%
$\sigma^2 = 1$	59%	56%	54%	56%	26%	54%
$\sigma^2 = 0.1$	71%	66%	65%	59%	46%	55%
$\sigma^2 = 0.01$	78%	79%	78%	64%	49%	60%
Inf^2Guard	77%	51%	80%	51%	46%	50%

Table 17: Inf^2Guard results against PIAs, where the attacker is unknown to the true (mean) aggregator and uses a substitute (max) one to aggregate the subset representations.

λ	Census		RSNA			CelebA		
	Utility	PIA Acc						
0	85%	48%	0	83%	42%	0	91%	40%
0.25	83%	45%	0.25	82%	24%	0.25	91%	22%
0.5	82%	44%	0.5	82%	21%	0.5	91%	15%
0.75	81%	28%	0.75	81%	15%	0.75	88%	9%
1	60%	25%	1	60%	14%	1	63%	9%

Table 18: Inf^2Guard results against DRAs with uniform perturbation distribution. A smaller SSIM or PSNR indicates better defense performance ($\lambda = 0.4$).

CIFAR10		
Scale ϵ	Utility	SSIM/PSNR
0	89.5%	0.78 / 15.97
1.25	85.7%	0.28 / 13.23
2.25	77.7%	0.24 / 12.34
3.25	64.9%	0.20 / 12.93

a larger model can better memorize the training data. Table 16 shows more DP results (vs varying ϵ 's) against MIAs. We can see Inf^2Guard obtains higher utility than DP methods under the same privacy protection performance.

More results on defending against PIAs: Figure 12- Figure 14 shows the t-SNE embeddings of Inf^2Guard against PIAs. Table 17 shows Inf^2Guard results against PIAs, where the attacker does not the true (mean) aggregator and use a substitute one (i.e., max-aggregator). We can see the attack performance is less effective and Inf^2Guard can yield (close to) random guessing attack performance (when $\gamma = 0.75$), with a slight utility loss. This implies the aggregator plays a critical role in designing effective PIAs against Inf^2Guard .

More results on defending against DRAs: Table 18 shows the Inf^2Guard results against DRAs, where the perturbation distribution is uniform distribution. We observe similar utility-privacy tradeoff in terms of the noise scale ϵ .

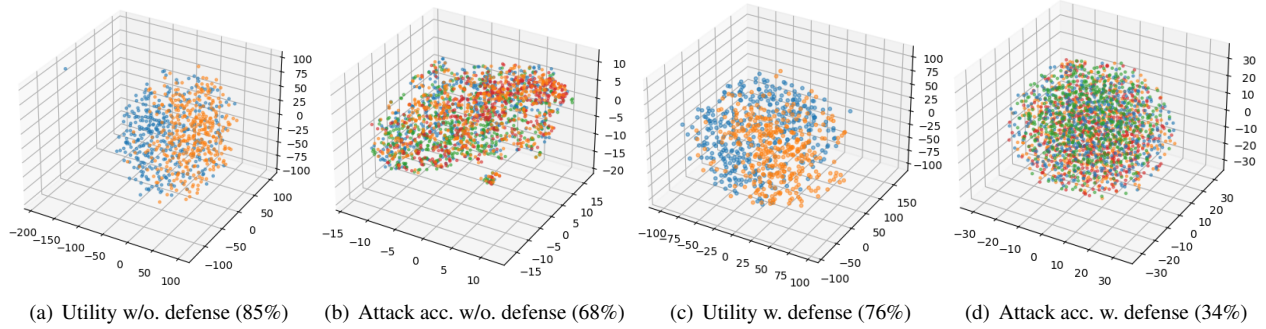


Figure 12: Inf^2Guard against PIAs: 3D t-SNE embeddings results on the learnt representation on Census Income. Each color indicates a label or a female ratio, and each point is a data representation in (a) and (c) or an aggregated representation in (b) and (d) of a subset in the learning task and in the privacy task, respectively. Same for the other two datasets.

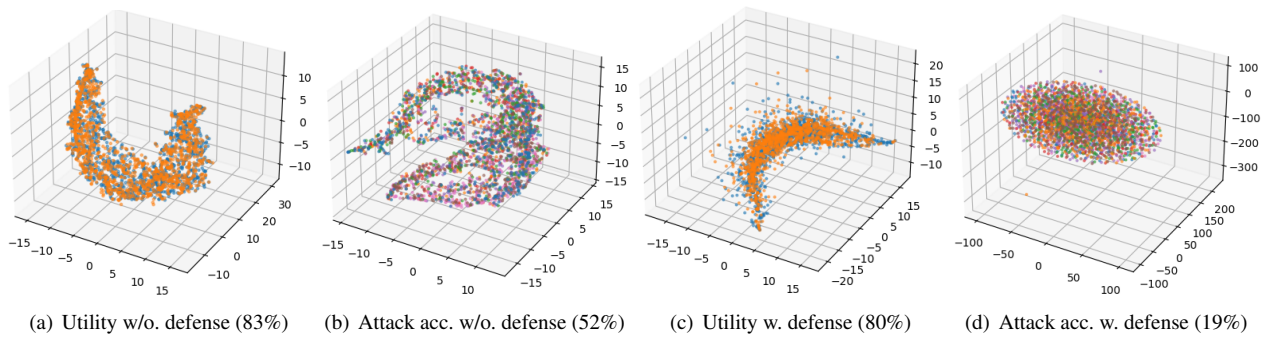


Figure 13: Inf^2Guard against PIAs: 3D t-SNE embeddings results on the learnt representation on RSNA Bone Age.

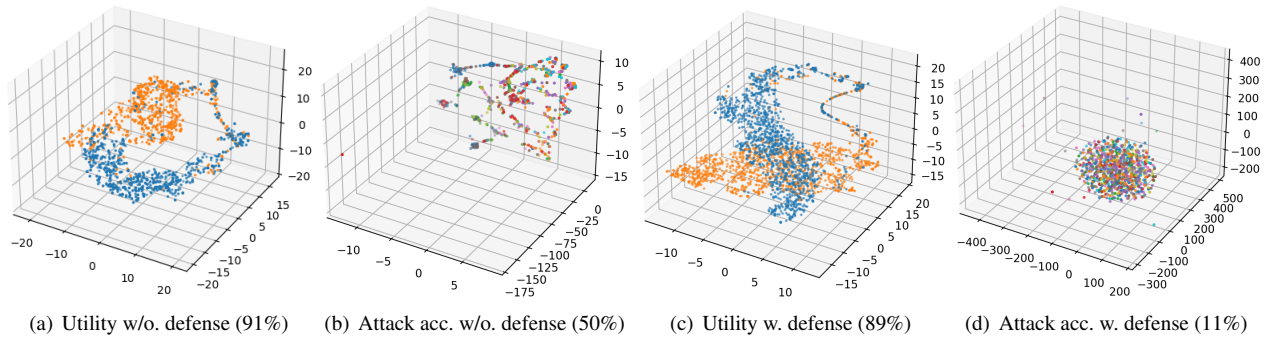


Figure 14: Inf^2Guard against PIAs: 3D t-SNE embeddings results on the learnt representation on CelebA.

D Optimal Solution of Inf^2Guard

Inf^2Guard involves training three (deep) neural networks whose loss functions are highly non-convex. To protect the data privacy, Inf^2Guard needs to solve a min-max adversary game, whose optimal solution could be *Nash Equilibrium*. However, finding Nash Equilibrium for highly non-convex functions can be a challenging problem, as traditional optimization techniques may not work effectively in such cases.